Turbulence and hypoxia contribute to dense biological scattering layers in Patagonian Fjord System.

Authors: Iván Pérez-Santos[1-2*], Leonardo Castro[2-3-4], Lauren Ross[5], Edwin Niklitschek[1], Nicolás Mayorga[1], Luis Cubillos[2-3], Mariano Gutierrez[6], Eduardo Escalona[2-3], Manuel Castillo[2-7], Nicolás Alegría[8] and Giovanni Daneri[2-9].

[1]Universidad de Los Lagos, Centro i~mar, Camino a Chinquihue km 6, Puerto Montt, Chile.

[2]COPAS Sur-Austral, Universidad de Concepción, Campus Concepción, Víctor Lamas 1290, Casilla 160-C, código postal: 4070043, Concepción, Chile.

[3]Departamento de Oceanografía, Universidad de Concepción, Campus Concepción, Víctor Lamas 1290, Casilla 160-C, código postal: 4070043, Concepción, Chile.

[4]Centro de Investigaciones de Altas Latitudes (IDEAL), Universidad Austral de Chile, Valdivia, Chile.

[5]Department of Civil and Environmental Engineering, University of Maine, 5711 Boardman Hall, Orono, ME 04469-5711.

[6]Universidad Nacional Federico Villareal, Facultad de Oceanografía, Pesquerías y Ciencias Alimentarias, Calle Francia 726, Miraflores, Lima, Perú.

[7]Centro de Observación Marino para Estudios de Riesgo en Ambientes Costeros, Facultad de Ciencias del Mar y de Recursos Naturales, Universidad de Valparaíso, Chile.

[8]Instituto de Investigaciones Pesqueras, Talcahuano, Chile.

[9]Centro de Investigaciones en Ecosistemas de la Patagonia (CIEP), Coyhaique, Chile.

***Corresponding author**: Iván Pérez-Santos, email: ivan.perez@ulagos.cl

Abstract

The aggregation of plankton species along fjords can be linked to physical properties and processes such as stratification, turbulence and oxygen concentration. The goal of this study is to determine how water column properties and turbulent mixing affect the horizontal and vertical distributions of macrozooplankton along the only north Patagonian Fjord known to date where hypoxic conditions occur in the water column. Acoustic Doppler Current Profiler moorings, scientific echo-sounder transects, and *in-situ* plankton abundance measurements were used to study macrozooplankton assemblages and migration patterns along Puyuhuapi Fjord and Jacaf Channel in Chilean Patagonia. The dissipation of turbulent kinetic energy was quantified through vertical microstructure profiles collected throughout time in areas with high macrozooplankton concentrations. The acoustic records and *in-situ* macrozooplankton data revealed diel vertical migrations (DVM) of siphonophores, chaetognaths and euphausiids. In particular, a dense biological backscattering layer was observed along Puyuhuapi Fjord between the surface and the top of the hypoxic boundary layer (~100 m), which limited the vertical distribution of most macrozooplankton and their DVM, generating a significant reduction of habitat. Aggregations of macrozooplankton and fishes were most abundant around a submarine sill in Jacaf Channel. In this location macrozooplankton were distributed throughout the water column (0 to ~200 m), with no evidence of a hypoxic boundary due to the intense mixing near the sill. In particular, turbulence measurements taken near the sill indicated high dissipation rates of turbulent kinetic energy (ε ~10^{-5} W kg^{-1}) and vertical diapycnal eddy diffusivity (K_ρ ~10^{-3} m^2 s^{-1}). The elevated vertical mixing ensures that the water column is well oxygenated (3-6 mL L^{-1}, 60-80 % saturation), creating a suitable environment for macrozooplankton and fish aggregations. Turbulence induced by tidal flow over the sill apparently enhances the interchange of nutrients, oxygen concentrations, and create a fruitful environment for many marine species, where prey-predator relationship might be favored.

Keywords: turbulence, hypoxia, Acoustic data, macrozooplankton, scientific echo-sounder, Patagonian fjords, sill exchange.

1 Introduction

Spatial and temporal variability of plankton assemblages have been linked to oceanographic features and processes such as water column stratification, tidal mixing and turbulence, frontal structures, advection, and secondary circulation in estuaries and fjords (Govoni et al., 1989; Rodriquez et al., 1999; Lee et al., 2005; Lough and Manning, 2001; Munk et al., 2002; Meerhoff et al., 2013; Meerhoff et al., 2015). In fjords, residual flows resemble typical estuarine gravitational circulation with landward flow at depth and seaward flow at the surface. It has been found that residual flows in fjords can retain planktonic larvae inside the system (Dyer, 1997; North and Houde, 2001, 2004; Meerhoff et al., 2015). Another recent study has shown that advection can influence the import and export of zooplankton in a fjord depending on the depth at which the zooplankton are located, which can potentially affect the community composition, biomass, productivity and distribution of zooplankton in the fjord (Basedow et al., 2004). Moreover, horizontal mixing of along-channel density gradients has been shown to induce lateral circulation (Farmer and Feeland, 1983), which in turn affects larval distributions in fjord systems (Meerhoff et al., 2015).

Other recent studies have investigated how tidally asymmetries in mixing, and thus tidal variations in stratification, affects ichthyoplankton and zooplankton assemblages (Pérez et al., 1977; Nixon et al. 1979; Oviatt, 1981, Lee et al., 2005). Lee et al., (2005) found that variations in stratification throughout a tidal cycle affected both overall abundance and species composition of zooplankton in the Irish Sea. However, they did not have the tools to relate the hydrodynamic and hydrographic variability of this region to vertical and horizontal distributions of fish larvae and zooplankton. Another study by Oviatt (1981) found that zooplankton concentrations were lower in laboratory tanks than in nature (Narragansett Bay, USA). Since this was not due to the physical action of mixing (induced by paddles in the tank), they hypothesized that tank confinement and turbulence had broken down vertical segregation between adults and juveniles, resulting in increased cannibalism. While vertical segregation of zooplankton groups, probably related to different trophic guilds, has been confirmed by several studies (e.g. Haury et al., 1990), this segregation can be reduced by turbulent processes enhancing contact between prey and predators (Visser and Stips 2002; Visser et al., 2009). For instance, available theoretical models predict optimal prey consumption at dissipation rates of turbulent kinetic energy (ε) between 10^{-6} and 10^{-4} W kg^{-1} (Lewis and Pedley, 2001). In fjords, topographic conditions are extremely irregular (Inall and

Gillibrand, 2010), inducing high turbulence and enhanced vertical mixing, particularly at sills (Klymak and Gregg 2004; Whitney et al., 2014). However, enhanced productivity, oxygenation, and/or local retention may occur at these same highly turbulent areas. For example, turbulence is known to mix freshwater inflow with deep, dense ocean water, allowing for oxygenation of the deeper layers (MacCready et al., 2002; Peters and Bokhorst, 2001) and turbulent these eddies can impact phytoplankton bloom growth (Cloern, 1991; Koseff et al., 1993). Therefore, additional field studies are needed to confirm the relationship between mixing-inducing physical forcing, such as wind or advection, and vertical abundance patterns and species composition in fjords and other estuarine systems. One of the principal questions that will be address in this study is: what is the contribution of turbulence to the mixing of fjord water column properties (e.g., Temperature, salinity and dissolved oxygen) and to the aggregation of macrozooplankton at certain depths (scattering layers) along north Patagonian fjords and channels, emphasizing the role of sills in some locations (e.g., Jacaf Channel, Fig. 1)?

Dissolved oxygen (DO) is the most important dissolved gas in the ocean as it sustains marine life and ensures ecosystems health. Most of the world's oceans are oxygenated, however there are some regions of low DO, referred to as hypoxic zones and if their DO concentrations are equal or close to 0 mL L^{-1} they are known as "Dead zones" (Díaz et al., 2001; Ekau et al., 2010; Hauss et al., 2016). Throughout the world's oceans there exist areas where hypoxic conditions are permanent and where the DO is significantly lower than well-oxygenated areas (e.g., <20 µM or 0.31 mL L^{-1}). These areas are known as Oxygen Minimum Zones (OMZs) and due to the upwelling associated with them; they experience elevated primary production at the surface (Mass et al., 2014; Hauss et al., 2016; Seibel et al., 2016). The major ocean OMZs are located in the Eastern South and North Pacific, the Arabian Sea, Bay of Bengal (Indian Ocean), West Bering Sea, the Gulf of Alaska and the Eastern North Atlantic, covering around 8% of the total ocean (~30 million km^2) (Paulmier and Ruiz-Pino, 2009; Fuenzalida et al., 2009; Hauss et al., 2016). The Eastern South Pacific OMZ (ESP-OMZ), present along the Chilean coast, represents an area of 9.8 million km^2 (2.6 % of the total ocean) (Fuenzalida et al., 2009). Even the ESP-OMZ decreased and disappeared south of ~37° S, however water with low DO (2-3 mL L^{-1}), associated with the Equatorial Subsurface Water (ESSW), is still present up to 44° S (Silva et al., 2009). The ESSW water mass

infiltrates Patagonian fjords and channels and moves northward and southward (41.5°-44° S) depending on the marine topography (Sievers and Silva, 2008).

Hypoxic conditions (< 2 mL L^{-1}) have been detected in four regions of Patagonian (Puyuhuapi Fjord, Jacaf Channel, Aysén Fjord and the Almirante Montt Gulf), and in each region the oxygen depleted zones are mainly located at the fjords head and down to 100 m depth (Silva and Vargas, 2014; Schneider et al., 2014). Some of the main contributors to hypoxia in Patagonian fjords and channels have been found to be (1) water column stratification causing separation between poorly oxygenated bottom water and oxygenated surface waters, (2) DO consumption by degradation of organic matter (autochthonous and allochthonous), (3) low ventilation due to the presence of deep bathymetric micro basins, (4) advection of the ESSW and (5) anthropogenic activities such as industrial and sewage discharge, riverine inputs of nutrients, agriculture activities, aquaculture, etc. (Sievers and Silva, 2008; Silva and Vargas, 2014; Schneider et al., 2014).

Hypoxia is known to have a significant impact on plankton distribution and development, hence on the health of the ecosystem as a whole (Ekau et al., 2010; Mass et al., 2014; Hauss et al.,2016; Seibel et al., 2016). Some species can tolerate hypoxic water, e.g., smaller species, euphausiids and jellyfish can live in under 30% oxygen saturation and dissolved oxygen of 1.6 mL L^{-1}. Other taxa, such as some copepods and fishes, may be more sensitive to hypoxia and have preference for oxygen saturations of 50-100% and DO concentrations of 2.6-5.2 mL L^{-1} (Ekau et al., 2010; Mass et al., 2014; Hauss et al., 2016; Seibel et al., 2016). The sensitivity of species to tolerate different oxygen concentrations, however, may vary among organisms from different environments, e.g., coastal upwelling zone, fjords systems and OMZ. Although hypoxic conditions have been detected in four regions of Patagonia (Silva and Vargas, 2014; Schneider et al., 2014) no relationship has been determined with the zooplankton species that inhabit this ecosystem. Therefore, the second question that motivates this study is: How do hypoxic conditions affect the distribution and aggregation of macrozooplankton species? This question will be addressed by investigating Puyuhuapi Fjord and Jacaf Channel, two of the four hypoxic systems in Patagonia.

In Patagonian fjords, a comprehensive description of zooplankton distribution patterns has been provided by Palma (2008), considering a total of 220 *in-situ* plankton samples, from a number of depth strata between the surface and ~200 m. Main zooplankton groups included siphonophores, chaetognaths, cladocerans, copepods and euphausiids. Although a positive

north to south gradient in the abundance of major zooplankton species was found, potential relationships between the vertical distributions and environmental variables were not deeply assessed. A later study by Landaeta et al., (2013) investigated the vertical distribution of microzooplankton and fish larvae in Steffen fjord (47.4° S) at four depth strata (200-50 m, 50-25 m, 25-10 m and 10-0 m depth) during November 2008. Copepod nauplii and copepodites of *Acartia tonsa* together with *Maurolicus parvipinnis* fish larvae were observed around the pycnocline region, suggesting that the vertical structure of the water column might play a role in larval fish distribution. More recently, studies on zoo- and ichthyoplankton vertical distributions in Reloncaví Fjord revealed that DVM timing might be modified by the tidal regime which is particularly strong in this area (Castro et al., 2014). However, none of these studies provided explicit assessments of the relationships between the vertical distribution of zooplankton and turbulent mixing or water column properties.

Most studies carried out in Chilean coastal waters, including those mentioned above, have relied on plankton nets and other collecting devices (pumps) deployed in single locations (fixed stations). An alternate approach is to use acoustic techniques, which can provide high resolution data on zooplankton DVM patterns (Valle-Levinson et al., 2014; Días-Astudillo et al., 2017) and segregation patterns throughout the water column (Sato 2013; Sato et al., 2016). For instance, DVM patterns of dense krill aggregations have been detected using Acoustic Doppler Current profilers (ADCP) moored around the Antarctic Peninsula, the Kattegat Channel and off Funka Bay, Japan (Buchholz et al., 1995; Lee et al., 2004; Zhou and Dorland 2004; Brierley et al., 2006). In Chilean fjords, ADCPs have been used to identify changes in vertical distribution and DVM patterns of zooplankton (e.g., from normal diel to twilight vertical migrations) over several months in Reloncaví Fjord (Valle-Levinson et al., 2014). These studies, although novel at describing temporal variations in zooplankton patterns, focused mainly on the behavior of particular species, but again did not consider how the vertical distribution of zooplankton is modified by water column conditions (e.g., temperature, salinity, oxygen and turbulence).

Compared to ADCPs, scientific echo-sounders are characterized by narrower beam angles, lower frequencies and longer ranges. They have also been used to provide valuable qualitative and quantitative information on various aquatic species and communities, from zooplankton to large predators (Ballón et al., 2011). Overall, macrozooplankton can be acoustically identified and virtually separated from other organisms, such as fish, by

considering their acoustic properties (Kloser et al., 2002; Logerwell and Wilson, 2004; Mosteiro et al., 2004; Simmonds and MacLennan, 2005). Although the use of several frequencies does not necessarily increase precision (Horne and Jech, 1999), the use of at least two frequencies (38 and 120 kHz) is currently a standard practice in zooplankton studies as identification methods developed by Ballón et al., (2011) and others can be utilized.

The present study aims to evaluate the effects of water column properties, such as dissolved oxygen and turbulent mixing, on the vertical distribution of dominant macrozooplankton groups along a Patagonian Fjord system. To achieve this goal ADCP and scientific echo-sounder data were combined with biological observations from *in-situ* stratified zooplankton samples and water column measurements from microstructure profilers and conductivity-temperature-depth-oxygen (CTDO) profilers. According to the information presented in this section, the principal hypotheses of this manuscript are: (1) the pervasive hypoxic layer existing in the Puyuhuapi Fjord limits DVM and overall distribution of macrozooplankton to the first 100 m depth of the water column, reducing the habitat of these species and (2) the higher turbulence originated by the tidal regime around sills favor the mixing of the water column, deepen the hypoxic layer, injects nutrients and, thus, increases primary production. Therefore, macrozooplankton exhibits higher densities and extends deeper in the water column around submarine sills.

2 Study Area

Patagonian fjords extend from 41° S to 56° S, and are typically deep and narrow as a result of their formation during glacial progression. Their hydrography is characterized by two vertical layers, consisting of a low salinity surface layer in the first ten meters of the water column (resulting from rainfall and glacial melt) that overlays a subsurface salty layer originated in the Pacific Ocean (Silva and Calvete, 2002; Pérez-Santos et al., 2014). Fjord systems play an important role in primary production and carbon cycling by providing a zone where energy and particulate material are exchanged between land and marine ecosystems (Gattuso et al., 1998). The principal nutrient (nitrate) is supplied to these fjords by oceanic transport, and particularly through the intrusion of Sub Antarctic Water (SAAW), a water mass that may also transport some species of zooplankton (González et al., 2011; 2013).

Puyuhuapi Fjord and Jacaf Channel are representative examples of the Patagonian Fjord Systems. The main connection of Puyuhuapi Fjord with oceanic waters is via its southern mouth. Although a second connection to oceanic water exists via Jacaf Channel, interchange here is limited by the shallow Jacaf Channel sill, which is 50 m deep and 6 km long. Its main freshwater input (the Cisnes River) meets the fjord half way between its head and mouth (Fig.1). Jacaf Channel is well known for its great depth (> 400 m) around its connection to the Moraleda Channel, which contrasts with its very shallow sill near its connection with Puyuhuapi Fjord (Fig. 1). Seasonal hydrographic measurements along Puyuhuapi Fjord have shown a stratified water column except in late winter, when the water column became partially mixed due to a reduction in freshwater supply from rainfall and glacial melting (Schneider et al., 2014). Hypoxic conditions have been detected in Puyuhuapi Fjord below 100 m depth, where oxygen concentrations have been found to be as low as 1-2 mL L^{-1} (Schneider et al., 2014; Pérez-Santos, 2017). This observed oxygen depletion could be caused by limited ventilation due to shallow sills, or by the input of low-oxygen Equatorial Subsurface Water into the fjord (Silva and Vargas, 2014; Schneider et al., 2014). Puyuhuapi Fjord is the only northwestern Patagonian fjord known to experience such extreme hypoxic conditions. At the same time, it is an area where intense aquaculture activities have been recently developed, which reinforces the need of this study.

The study area offers an excellent opportunity for studying the impact of deep hypoxia upon macrozooplankton distribution and behavior, considering the continued increase of hypoxic regions around the world (Breitburg et al., 2018). Moreover, the presence of a sill in Jacaf Channel, in the vicinity of its connection to the Puyuhuapi Fjord, opens the possibility to investigate the influence of vertical mixing (Farmer and Freeland, 1983; Inall and Gillibrand, 2010) upon water quality, especially upon dissolved oxygen concentration, injection of nutrients from subsurface oxygen rich layers, enhancement of primary production and, finally, upon the density of different zooplankton species (Pantoja et al., 2011). Furthermore, the location of an oceanographic buoy in the northern part of Puyuhuapi Fjord (Schneider et al., 2014) is a useful platform to carry out *in-situ* experiments combined with oceanographic moorings.

3 Data collection and methodology

3.1 Water column properties

Hydrographic surveys were conducted during May and November 2013 and January and August 2014 in Puyuhuapi Fjord and Jacaf Channel (Fig. 2, Table 1). These profiles were obtained with a Seabird 25 CTDO, sampling at 8 Hz with a descent rate of ~1 m s^{-1}. The data collected, whose nominal vertical resolution was ~12 cm, were averaged into 1 m bins, following Seabird recommendations. The conservative temperature (˚C) and absolute salinity (g kg^{-1}) were calculated according to the Thermodynamic Equation of Seawater 2010 (COI et al., 2010). Additionally, nitrate samples were taken using a Niskin bottle at various depths and analyzed spectrophotometrically following the methods of Strickland and Parsons (1968). To validate CTDO oxygen measurements, *in-situ* oxygen samples were analyzed using the Winkler method (Strickland and Parsons, 1968), carried out using a Metrohom burette (Dosimat plus 865) and an automatic visual end-point detection (AULOX Measurement System).

Microstructure measurements were collected using a Vertical Microstructure Profiler (VMP-250, Rockland Scientific, Inc.). The VMP-250 is equipped with two airfoil shear probes and two fast response FP07 thermistors, which allowed for data recording at 512 Hz with a descending free fall speed of ~0.7 m s^{-1}. The micro-shear measurements permitted a direct measurement of the dissipation rate of turbulent kinetic energy (ε) for isotropic turbulence, according to Lueck et al., (2002), Eq. (1),

$$\varepsilon = 7.5\,\nu\overline{\left(\frac{\partial u'}{\partial z}\right)^2} \qquad (1)$$

where, ν is the kinematic viscosity, u is the horizontal velocity, z is the vertical coordinate axis and therefore $\overline{\left(\frac{\partial u'}{\partial z}\right)^2}$ is the shear variance.

Using the values of ε, the diapycnal eddy diffusivity (K_ρ) was calculated. The most used formulation was proposed by Osborn (1980),

$$K_\rho = \Gamma\,\frac{\varepsilon}{N^2}, \qquad (2)$$

where Γ is the mixing efficiency, generally set to 0.2 (Thorpe 2005), and N is the buoyancy frequency. Shih et al. (2005) noted that when the ratio $\varepsilon/\nu N^2$ is greater than 100, Eq. (2) results in an overestimation. Therefore, they proposed a new parameterization for this case given by:

$$K_\rho = 2\nu\left(\frac{\varepsilon}{\nu N^2}\right)^{1/2}. \qquad (3)$$

More recently, Cuypers et al. (2011) used Eq. (3) when $\varepsilon/\nu N^2 > 100$, Eq. (2) when $7 < \varepsilon/\nu N^2 < 100$, and considered null eddy diffusivity when $\varepsilon/\nu N^2 < 7$. This approach was followed in this study. The correlation between the dissipation rate of turbulent kinetic energy and the abundance of major zooplankton groups throughout the water column was accomplished by using a quadratic polynomial curve fit between these data sets (explained in detail in section 4.6). These analyses were only applied to measurements collected at the fixed station in Puyuhuapi Fjord, because the VMP-250 was not available during the measurement campaign in Jacaf Channel.

3.2 Acoustic data

Three types of acoustic data were collected: ADCP, single-frequency echo-sounder and dual-frequency echo-sounder data. ADCP measurements were obtained with two 307.7 kHz Teledyne RDI Workhorse ADCPs, moored upwards at depths of ~50 m (ADCP-1) and ~100 m (ADCP-2), both moored at the same location in north-central Puyuhuapi Fjord but during different time periods (Table 1, Fig. 1). Data were collected hourly with a vertical bin size of 1 m, over periods of austral autumn (ADCP-1: May, 2013) and spring-summer (ADCP-2: January 2014). During the final ADCP-2 mooring deployment, single-frequency data were also collected along the Puyuhuapi Fjord using a SIMRAD EK60 scientific echo-sounder, running a 38 kHz transducer (ES38B), during daytime and nighttime hours, from January 22-25, 2014 (black line in Fig. 1). These ADCP and single-frequency echo-sounder measurements were complemented by *in-situ* zooplankton sampling (see section 3.3 for details) carried out on January 23-24, 2014, at a fixed station close to the ADCP mooring location, over a period of 36 hours (Fig. 1).

A second scientific campaign was conducted on August 17th and 18th, 2014, which included a dual-frequency echo-sounder survey and a thrid ADCP mooring (ADCP-3) located in Jacaf Channel. This time, the echo-sounder survey coverage was extended to eastern Jacaf Channel (Fig. 1, red line) and a second 120 kHz transducer (ES120-7C) was added to the 38 kHz transducer used in the first survey. Several day/night transects were completed across Puyuhuapi Fjord and Jacaf Channel, with special attention paid to Jacaf sill (only the most representative echograms were showed in figures 5, 7 and 8). To determine the statistical relationship (R^2) between acoustic data from the 38 kHz echo-sounder with hydrographic properties of the fjords (temperature, salinity and dissolved oxygen), a quadratic polynomial

curve was also applied between these data sets. During this survey, two RDI Workhorse ADCP was 614.4 kHz frequency (referenced hereafter as ADCP-3) and was moored at ~30 m depth in the vicinity of the Jacaf sill. The near-surface placement of ADCP-3 allowed for near-surface currents to be adequately quantified.

Vessel speed during all echo-sounder surveys was maintained between 8 and 10 knots. Echo-sounders were operated using a variable ping rate 0.3-2.0 ping s^{-1}, pulse duration of 1.024 milliseconds and output powers of 2 kW and 0.5 kW for the 38 and 120 kHz frequencies, respectively. Calibration was made using copper spheres and standard procedures (Foote et al., 1987).

3.2.1 Echo-sounder data analysis

Post-processing of echo-sounder data was performed in Echoview (Myriax inc, Tasmania, https://www.echoview.com/), where noisy data considered as those collected with weak pings, in blind areas, in the near field, with background noise or subjected to rainbow phenomenon were regarded as "bad data" and were eliminated. After this initial scrutiny and filtering step, all single-frequency echoes (38 kHz, Campaign 1) of intensity >-110 dB were considered and treated as a single "biological backscattering" class, which pooled all biological groups being present in the study area. Dual-frequency echoes, however, were classified into three different groups following Ballón et al., (2010). These authors built an algorithm, freely distributed as an Echoview template ("FishZpkPeru38&120.evi"), which uses both mean volume backscattering (MVBS) differences ($\Delta MVBS$) and summations ($\sum MVBS$) between 38 and 120 kHz to discriminate echoes into three different biological backscattering classes: fish and two macrozooplankton groups (macrozooplankton or "fluid-like" and gelatinous or "blue noise" organisms). The fluid-like group follows a sphere model (Holliday & Pieper, 1995) considered appropriate to represent cylindrical and spherical shapes, including euphausiids and large copepods, which are dominant macrozooplankton groups off Peru and Chile (Ayon et al., 2008). The algorithm is considered to be useful for 38 and 120 kHz data from targets whose radius is ≥0.5 mm and has a dB difference of 2-19 dB (Ballón et al., 2010 and 2011).

Given physical limitations imposed by near field and sound absorption effects related to the echo-sounder frequencies used (38 and 120 kHz), we defined and limited our analyses to an effective sampling range between 5 and 250 m. Absorption is greater for the 120 kHz

frequency, which exhibits the shortest range, but has a greater vertical resolution than 38 kHz echo-sounder. The 38 kHz frequency, on the other hand, exhibits a much longer range (>1000 m), but limited resolution regarding small zooplankton scatterers., It has been shown, however, to be efficient for studying macrozooplankton distributions of siphonophores, chaetognaths and euphausiids (Mair et al., 2005; Cade and Benoit-Bird, 2015; Ariza et al., 2016).

Volume backscattering strength (S_v, dB re 1 m^{-1}) values from the single-frequency and from each of the three dual-frequency virtual echograms were integrated and re-scaled into the customary index "nautical area scattering coefficient" (NASC, in units of m^2 n mi^2), using a grid of 20 m (depth) by 50 m (distance). Since NASC lies on the linear domain, it can be considered proportional to and suitable for indexing targets abundance (Ballón et al., 2011).

Quadratic polynomial models were fit to assess the statistical relationship (R^2) between biological scattering (single-frequency integrated data) and the hydrographic variables measured in each fjord (temperature, salinity and dissolved oxygen).

3.2.2 Acoustic data analysis from ADCPs

ADCP echo intensity was converted to mean volume backscattering strength (S_v, dB re 1 m^{-1}), as done for scientific echo-sounder data, following the conversion formula:

$$S_v = C + 10log[(Tx + 273.16)R^2] - L_{DBW}\text{-}P_{DBW}+2\alpha R + K_c(E - E_r) \quad (4)$$

where, C is a sonar-configuration scaling factor (-148.2 dB for the Workhorse Sentinel), T_x is the temperature at the transducer (°C), L_{DBW} is $\log_{10}$(transmit-pulse length, L=8.13 m), P_{DBW} is $\log_{10}$(output power, 15.5 W), α is the absorption coefficient (dB m^{-1}), K_c is a beam-specific sensitivity coefficient (supplied by the manufacturer as 0.45), E is the recorded AGC (automatic gain control), and E_r is the minimum AGC recorded (40 dB for ADCP-1 and 41 dB for ADCP-2). The beam-average of the AGC for the 4 transducers was used to obtain optimal results following the procedure in Brierley et al. (2006). Finally, R is the slant range to the sample bin (m), which uses the vertical depth as a correction (Lee et al., (2004)). Therefore, R is expressed as,

$$R = \frac{b+\frac{L+d}{2}+\left((n-1)d\right)+(d/4)}{\cos\zeta}\frac{\bar{c}}{c_I} \quad (5)$$

where b is the blanking distance (3.23 m), L is the transmit pulse length (8.13 m), d is the length of the depth cell (1 m), n is the depth cell number of the particular scattering layer being measured, ζ is the beam angle (20°), $\bar{c}$ is the average sound speed from the transducer to

the depth cell (1453 m s^{-1}) and c_1 is the nominal sound speed used by the instrument (1454 m s^{-1}).

3.3 In-situ zooplankton sampling

In situ mesozooplankton samples were collected with a WP2 net (60 cm diameter mouth opening, 300 µm mesh, flowmeter mounted in the net frame) towed vertically from 50 m to the surface in May 2013, and with a Tucker trawl (1 m^2 mouth opening, 300 µm mesh with flowmeter) used to obtain stratified oblique tows in January 2014 and August 2014 (Table 1). All samples were preserved in a 5% formaldehyde solution. Zooplankton abundances were standardized to individuals per m^3 of filtered seawater. WP2 vertical tows consisted of 5 depth intervals from surface to 50 m, every 10 m (0-10, 10-20, 20-30, 30-40, 40-50 m).

Stratified Tucker tows considered four depth strata: 0-10 m, 10-20 m, 20-50 m, 50-100 m in the Puyuhuapi Fjord. In Jacaf Channel, the stratified sampling included five depth strata: 0-10 m, 10-20 m, 20-50 m, 50-100 m and 100-150 m. The hauling speed for both nets was between 2-3 knots. Sampling occurred during a 36-h period every 3 h from January 22-24, 2014 (Puyuhuapi Fjord) and every 5-6 h from August 18-19, 2016 (Jacaf Channel) (Fig. 1, red dots). At all sites and dates, zooplankter's were identified, sorted into functional groups, measured (length) and classified into size-classes using a 5 mm length threshold. To determine the correlation (R^2) between the S_v records from the 38 kHz transducer and the major macrozooplankton groups (Siphonophores, Chaetognaths and Euphausiids), a quadratic polynomial curve was also applied between these data sets (further details in section 4.3).

3.4 Tidal harmonic analysis

The tidal constituents were computed using HOBO U20 water level loggers and the pressure sensor from ADCP-3 (Table 1-2, Fig. 1). A tidal harmonic analysis was applied to the sea level time series according to Pawlowicz et al., (2002), which considers the algorithms of Godin (1972, 1988) and Foreman (1977, 1978). We classified tides by the dominant period of the observed tide based on the form factor (F), defined by the ratio between the sum of the amplitudes of the two main diurnal constituents (larger lunar declinational, O_1 and luni-solar declinational, K_1) and the sum of the amplitudes of the two main semi-diurnal constituents (principal lunar, M_2 and principal solar, S_2), $F = (O_1+K_1)/(M_2+S_2)$ (Bearman , 1989; where, F < 0.25 semi-diurnal, 0.25 < F< 1.5 Mixed semi-diurnal and F > 3.0 diurnal).

4. Results

4.1 Hydrographic features

Temperature profiles collected in Puyuhuapi Fjord and Jacaf Channel showed similar structure during the winter and summer campaigns (Fig. 2, a-b). The largest temperature gradients were found between the surface and ~70 m depth, ranging from 8.5° C to 17° C. A thin, fresh layer (salinity values varied from 11 to 29 g kg^{-1}) was found in the first ~10 m of the water column below which salinity varied little (29 to ~34.2 g kg^{-1}), as result of the presence of Modified Sub-Antarctic water (MSAAW, salinity between 31 and 33 g kg^{-1}), the Sub-Antarctic Water (SAAW, salinity between 33 and 33.8 g kg^{-1}) and the Equatorial Subsurface Water (ESSW, salinity>33.8 g kg^{-1}) (Fig. 2, c-d). Hypoxic conditions (dissolved oxygen below 2 mL L^{-1} and ~30 % saturation) were detected in Puyuhuapi Fjord below 100 m depth, with oxygen concentration between 1-2 mL L^{-1} (Fig. 2e). Deep water in Jacaf Channel was more ventilated, with dissolved oxygen values above hypoxic conditions throughout the water column (Fig. 2f). The hypoxic layer was located over the depth range of the Equatorial Subsurface Water (ESSW) and oxygen rich water (3-6 mL L^{-1}) was observed at depths occupied by MSAAW and SAAW. Below 10 m depth, high nitrate concentrations were measured in Puyuhuapi Fjord, but concentrations in the winter (August 2014) were higher than in fall (May 2013) and summer (January 2014) (Fig. 2 g). Along with the in-situ hydrographic sampling, in-situ zooplankton samples were collected and will now be discussed.

4.2 ADCP Acoustic data and *in-situ* zooplankton samples

Volume backscatter (S_v) from ADCP-1 (50 m depth, May 2013) showed large variability, ranging from high (-90 to -75 dB re 1 m^{-1}) to low (-115 to -100 dB re 1 m^{-1}) (Fig. 3a). The highest S_v values (>-90 dB re 1 m^{-1}) were recorded during the night hours (~18:00 to ~07:00, local time; with all remaining times for in-situ sampling expressed in local time), while minimum S_v values were observed in the daytime (~07:00 to ~18:00) suggesting vertically migrating organisms from deeper waters (below ADCP-1 mooring depth of 50 m) migrate upwards during nighttime hours. From the *in-situ* measurements of macrozooplankton collected at various depth strata in May 2013, the most abundant groups were siphonophores, chaetognaths and medusae (Fig. 3c-f). A marked change in vertical distribution and in total abundance of the macrozooplankton groups in the water column was observed from the first

441 sampling hour (Fig. 3c) to the night sampling time (~18:00 h), revealing the start of the
442 nocturnal migration to the surface (Fig. 3d) coincident with a DVM pattern as seen in the
443 ADCP-1 backscatter data (Fig. 3a-b).
444 Data from the ADCP-2 mooring (positioned deeper but at the same location as ADCP-
445 1) from January 22-24, 2014 also showed a strong macrozooplankton DVM pattern, which
446 extended down to ~100 m depth (Fig. 4a). During daylight hours (8:00-18:00), dense
447 aggregations were observed between 80-100 m depth, which started to ascend from 18:00 to
448 21:00, concentrated close to the surface at night, and began to descend at ~06:00. In-situ
449 stratified sampling showed the most abundant macrozooplankton groups were euphausiids,
450 siphonophores, chaetognaths, decapods and medusae (Fig. 4 b-f). Euphausiids and
451 siphonophores showed higher abundance close to surface layer (10-20 m) during night hours
452 (Fig. 4c and Fig. 4f) and at deeper layers during the daytime (Fig. 4d and Fig. 4e). However,
453 euphausiids showed the clearest diel vertical migration with maximum abundance between
454 10-20 m layer during night hours, and at ~100 m depth during the daytime (Fig. 4c-f). The in-
455 situ zooplankton samples were complemented by echo-sounder measurements collected along
456 the fjord systems during the summertime and the wintertime. These measurements will now
457 be discussed.
458
459 **4.3 Echo-sounder data**
460 **4.3.1 Summertime single-frequency survey**
461 The volume backscatter during the summer months overall showed DVM of all
462 macrozooplankton species and a downward migration limit of ~100 m depth due to presence
463 of hypoxic conditions below this depth. Summer daytime S_v values along the Puyuhuapi Fjord
464 averaged -89.1 ±7 dB re 1 m^{-1} and ranged between -110 and -77.3 dB re 1 m^{-1}, from the
465 mouth to the head of the Puyuhuapi fjord (Fig. 5a). Most biological backscatter was
466 concentrated in the first 100 m of the water column, matching ADCP-2 results, which showed
467 an increase in backscattering towards 100 m depth (Fig. 4a and 5a). Highest daytime NASC
468 values were found around 80 m (above the hypoxic layer), reaching values of 3-3.5 m^2 n mi^2
469 (Fig. 5b). Although some backscatter occurred within the hypoxic layer (below ~120 m
470 depth), all dense aggregations were observed above it (Fig. 5e).
471 Summer nighttime biological backscattering along the Puyuhuapi Fjord (Fig. 5c)
472 showed maximum S_v values near the surface, suggesting an ascending vertical migration of all

biological backscatter. NASC profiles also showed both an increase in maximum abundances and a shift in the vertical position of the maximum values from 60-80 m during daytime to 40-60 m depth during nighttime (Fig. 5d). Although the water column depth extended to ~300 m, all dense backscatter aggregations were observed above 100 m depth during both day and night time hours (Fig. 5a and c). As DO concentrations decreased from 2 mL L^{-1} to 1 mL L^{-1} below 100 m depth, biological scatterers in Puyuhuapi Fjord appeared to prefer oxygen concentrations between 3 and 7 mL L^{-1} (Fig. 5e). The correlation between S_v values and the observed density of different zooplankton groups (*in-situ* samples, >5mm) was high. Such correlations reached values of R^2=0.50, for siphonophores (Fig. 6a), R^2=0.48 for chaetognaths (Fig. 6b), and R^2=0.72 for euphausiids (Fig. 6c). The wintertime sampling showed similar findings but was able to capture more activity in the water column due to the use of two acoustic frequencies.

4.3.2 Wintertime dual-frequency surveys

Wintertime dual-frequency surveys data, carried out along Puyuhuapi Fjord and Jacaf Channel on August 17th (~35 km total transect length, Fig. 1), allowed separation of total backscatter into Fish, Fluid like (FL) and Blue noise (BN) groups (Fig. 7a-b). Total backscatter (S_v) in Puyuhuapi Fjord (0-18 km) showed elevated values in the first 100 m of the water column, but at slightly deeper depths (50-100 m) than in summer (Fig. 5), possibly due to bad weather conditions encountered on the sampling day. Greater intensity (-80 to -60 dB re 1 m^{-1}) and vertical distribution range (0-220 m) of biological backscattering values (S_v>-110 dB) were observed in Jacaf Channel, particularly around its sill (between km 18 and 32; Fig. 7). Particularly high intensities were attributed to BN and FL groups at either side of Jacaf Channel sill on both August 17th and 18th (Fig. 7 and 8). An important degree of vertical segregation between BN and FL groups was also observed along Jacaf Channel, with the first group concentrated between 100 and 140 m, while the second was between 120 and 200 m (Fig. 7 and 8).

Continuous acoustic sampling repeated over the Jacaf Channel sill confirmed the presence of two backscattering layers: one denser layer between 100-150 m and a second, less dense layer from 200 to 250 m (Fig. 8a, showed only the best echogram). *In-situ* zooplankton sampling along the Jacaf Channel sill (Fig. 9f) allowed the detection of the major macrozooplankton groups (e.g., chaetognaths, euphausiids and crustaceans) found during this

experiment (Fig. 9a-d). In general, all sampling stations were carried out during daytime, but station 4 coincided with the ascending moment of macrozooplankotn, and highlighted the presence of euphausiids during this time of vertical migration (Fig. 9d). Also, station 1 showed the dominance of crustaceans in the 0-10 m strata. Overall the *in-situ* zooplankton sampling and the echograms showed good agreement with the FL group (Fig. 9a-d). Furthermore, the elevated abundance of macrozooplankton groups (euphausiids and chaetognaths) found between 100-150 m depth during daytime hours (Fig. 9b-f) matched well with acoustic data for the fluid-like group (Fig. 8a), but in the case of BN group the macrozooplankton species were not clearly identified in the *in-situ* zooplankton sampling.

A moderate correlation was found between S_v values from Jacaf Channel and zooplankton density calculated from *in situ* samples (>5 mm), with R^2=0.42 for S_v vs. chaetognaths (Fig. 6d) and R^2=0.41 for S_v vs. euphausiids (Fig. 6e). Now the relationships between water column properties such as temperature, salinity and DO will be compared to the acoustic and in-situ macrozooplankton measurements.

4.4 Relationships between biological scattering and water column properties

To examine relationships between the distribution of biological scattering and water column properties, S_v values quantified from the 38 kHz acoustic profiler were matched to the consecutive time at which CTD and DO data were captured. This was done in Puyuhuapi Channel and Jacaf Channel during the summer and winter seasons, respectively. The relationship between water temperature and S_v was weak during summer (R^2=0.30) and winter (R^2=0.41), with maximum S_v values occurring between 8 and 10°C (Fig. 10a and 10b). A weak relationship was found between S_v and salinity in Puyuhuapi Fjord (R^2=0.29, Fig. 10c) and Jacaf Channel (R^2=0.35, Fig. 10d), with higher S_v values found in the MSAAW and SAAW water masses (salinity >31 g/kg). Both in Puyuhuapi Fjord and Jacaf Channel S_v with DO and oxygen saturation showed the highest R^2 values (R^2~0.6, Fig. 10e-h). Hence, only 20.4% of total S_v>-110 dB re 1 m^{-1} were in the hypoxic layer of Puyuhuapi Fjord, while just 1.2 % were in the hypoxic layer in Jacaf Channel (Fig. 10e-h). Now the TKE dissipation will be discussed to relate macrozooplankton assemblages to vertical mixing in the water column.

4.5 Tidal regime

The harmonic analysis carried out with the sea level time series obtained in Puyuhuapi Fjord and Jacaf Channel, denoted the dominance (in terms of amplitude) of the semi-diurnal constituents (M_2 and S_2; Table 2). Diurnal constituents (O_1 and K_1) were also important, specifically at the Jacaf ADCP-3 station located close to the Jacaf sill region (Table 2 and Fig 1). The contribution of diurnal constituents added the mixed character to the tidal regimen in the study area. The spectral analysis implemented at all sea level stations showed maximum energy in the semi-diurnal band (Table 2), with the highest spectral energy (57.29 m^2 cph^{-1}) at Jacaf sill (Jacaf ADCP-3 station), which could be due to the extreme convergence of the channel at this location accelerating the tidal flows.

4.6 Mixing process

Turbulence measurements collected with the VMP-250 microstructure profiler showed high dissipation rates of turbulent kinetic energy (ε) in the upper 20 m of the water column in Puyuhuapi Fjord and Jacaf Channel (Fig. 11). In this layer ε ranged from 10^{-7} to 10^{-5} W kg^{-1}. However, below this surface layer (<20 m depth) the highest values were obtained around Jacaf sill (ε=1.2×10^{-7} W kg^{-1}), as shown on 21 November 2013 at 140 m depth (Fig. 11 a). In Puyuhuapi Fjord TKE dissipation between 20-180 m was weak (10^{-10} to 10^{-7} W kg^{-1}), (Fig. 11c and 11e). The dissipation rates of turbulent kinetic energy are obtained by integrating the velocity shear spectrum at each respective depth bin up to the noise limit. The noise limit is determined by comparing the measured spectra to the theoretical Naysmyth Spectra and determining where the measurements begin to deviate from theory. To display how the estimates of ε were obtained at the Jacaf sill depth, the shear spectra are shown for VMP profiles collected at the Jacaf sill region (21 November 2013 at 140 m depth; Fig. 11b), and in Puyuhuapi Fjord on 22 November 2013 (at 140 m depth; Fig. 11d) and on 23 January 2014 (at 140 m depth; Fig. 11f).

In Puyuhuapi Fjord the correlation between ε and zooplankton S_v data (38 kHz, fixed station, January 2014) was high (R^2=0.65, Fig. 12a). In the same campaign, the *in-situ* macrozooplankton density (>5 mm) was also high correlated with ε values (R^2=0.79 for ε vs. siphonophores, R^2=0.66 for ε vs. chaetognaths, and R^2=0.77 for ε vs. euphausiids) (Fig 12b-d). Unfortunately, VMP data was not collected in Jacaf Channel in wintertime. In order to confirm the relationship between ε and various zooplankton species, additional turbulence

measurements were collected in November 2013 along Jacaf sill (Fig. 13a). Results showed strong velocity shear in the horizontal velocities (Fig. 13b) accompanied by high ε values (10^{-7} to 10^{-5} W kg^{-1}; Fig. 11c). Maximum ε was measured at the Jacaf-Puyuhuapi confluence (10 km along transect) at ~63 m depth where $\varepsilon = 1.9\times10^{-5}$ W kg^{-1}, (Fig. 13b; St. 164). The diapycnal eddy diffusivity (K_ρ) was also high in the same area with values of 10^{-4} to 10^{-3} m^2 s^{-1} (Fig. 13c).

5 Discussion

This study represents one of the first attempts to combine measurements of acoustics, stratified plankton sampling, microstructure profiles, and standard hydrographic profiles to investigate both the vertical distribution patterns of macrozooplankton and why these patterns exist in northwest Patagonian Fjords and other subantarctic latitudes. Three main findings resulted from this effort. First, DVM patterns of macrozooplankton became evident from all methodological approaches, at all study periods: May 2013, January 2014 and August 2014 (Fig. 3-5 and Fig. 7-9). Second, strong evidence arose showing macrozooplankton avoidance of hypoxic layers. And, third, a clear increment of macrozooplankton and fish aggregations around the Jacaf sill could be related to increased turbulence in this area.

5.1 Diel vertical migration patterns

Consistent evidence from multiple echo-sounder surveys, ADCP moorings and semi-continuous *in-situ* zooplankton measurements supported the existence of major circadian displacements of macrozooplankton during night hours between mid-depth (20-120 m) and subsurface waters in our study area. Similar DVM patterns have been found in Reloncaví Fjord (41.5° S), from 300 and 600 kHz ADCP data, by Valle-Levinson et al., (2014) and Días-Astudillo et al., (2017) using a 75 kHz acoustic device. Given a greater resolution, the later work was able to confirm that the DVM affected the whole water column of the fjord (~200 m). These studies found the presence of euphausiids, decapods, mesopelagic shrimps, copepods and other groups in the Reloncaví Fjord in July and November, 2006 (Valle-Levinson et al., 2014), as well as in July 2013 (Días-Astudillo et al., 2017). DVM is a common feature of many zooplankton groups, observed around the world using different ADCP and echo-sounders frequencies, e.g., at the Kattegat Channel (Buchholz et al., 1995), the northeast Atlantic (Heywood, 1996), the northwest coast of Baja California, Mexico

(Robinson and Gómez-Gutiérrez, 1998), the northeastern Gulf of Mexico (Ressler, 2002), the Antarctic Peninsula (Zhou and Dorland 2004), the Arabian Sea (Fielding et al., 2004), Funka Bay, Japan (Lee et al., 2004), south Georgia, in the Atlantic sector of Southern Ocean (Brierley et al., 2006) and Saanish Inlet, Britisch Columbia, Canada (Sato et al., 2013). The scattering layers observed in these studies highlight the abundances of the major zooplankton species, represented by: amphipods, euphausiids, siphonophores, chaetognaths, pteropods, crustaceans, small fish and gelatinous plankton. While most DVM patterns reported in these studies occurred between 0 and ~300 m depth, the deepest DVM patters were observed in the North-Atlantic Ocean, reaching depths ~1600 m (Van Haren and Compton, 2013).

DVM patterns of zooplankton are expected to be associated with diel changes in visible light within the photic zone (from surface to ~100 m). Thus, the zooplankton can avoid predators during daytime hours and have safe-feeding conditions at night. While only small irradiance levels, $<10^{-7}$ times surface levels, can be detected beyond 600 m (Van Haren and Compton, 2013; Sato et al., 2013 and 2016), zooplankton DVM can reach depths below 500 m (Van Haren and Compton, 2013). Moreover, zooplankton DVM occurs in Arctic fjords (e.g., the Kongsfjorden and Rijpfjorden fjords) even during the polar night, suggesting high sensitivity to very low levels of solar and/or lunar light (Berge et al., 2009). Since both Puyuhuapi Fjord and Jacaf Channel are not deeper than 300 m, enough light should reach the bottom layer and stimulate zooplankton DVM across the whole water column. However, our results show that zooplankton DVM (and distribution as discussed in the next section) was limited by the hypoxic boundary layer present in the Puyuhuapi Channel (~100 m; Fig. 5), providing indirect support to the idea that hypoxia may limit DVM in low-ventilated Patagonian fjords and elsewhere (Ekau et al., 2010; Mass et al., 2014; Hauss et al., 2016; Seibel et al., 2016).

5.2 Macrozooplankton avoidance of hypoxic waters

In Puyuhuapi Fjord, hypoxic conditions have been reported below ~100 m depth, all year round (Schneider et al., 2014; Silva and Vargas 2014), with sporadic deep ventilation events that increase the DO concentration from 1.4 to 2.8 mL L^{-1} (Pérez-Santos, 2017). These pervasive hypoxic conditions are not common in all Patagonian Fjords. For instance, seasonal hydrographic data from Reloncaví Fjord showed well ventilated conditions along the fjord, with deep, near-bottom DO values between 3-3.5 mL L^{-1} (Castillo et al., 2016).

In the current study, acoustic measurements revealed that most biological backscattering (S_v data) occurred above the hypoxic boundary layer (Fig. 5 and Fig. 10), which acted as a barrier to DVM and macrozooplankton distribution throughout the year. Similar findings were reported in Oslofjord, Norway, where hypoxic conditions dominated the water column beneath ~60 m depth, and no fish or krill were observed below this depth (Røstad and Kaartvedt, 2013). Moreover, in Eastern South Pacific OMZ, it has been previously reported that a number of copepod species and life-stages avoid hypoxic waters (Castro et al. 1993, Escribano et al. 2009), as well as for most gelatinous zooplankton groups (Pages et al. 2001; Giesecke and Gonzalez 2005; Escribano et al. 2009). In the same OMZ region, but further north in Peruvian waters, two diurnal scattering layers were observed, one over the OMZ and other, mainly composed by adults euphausiids, in the core of the OMZ (Ballón et al., 2011). Euphausiids, salps and myctophid fish were also observed in the core of Eastern Tropical North Pacific OMZ (Mass et al., 2014). Seibel et al., (2016) reported *Euphausia eximia* and *Nematoscelis gracilis* tolerance to hypoxic water and suggest this tolerance would enable these species to reduce their energy expenditure in at least 50% during their daytime migration.

The highest S_v values observed in Puyuhuapi Fjord, occurred at DO concentrations between 2 and 5 mL L^{-1}, while in Jacaf Channel between 3 to 6 mL L^{-1}. DO values of 3.5 mL L^{-1} and 4.5 mL L^{-1} seemed to represent appropriate conditions for most macrozooplankton species in Puyuhuapi Fjord and Jacaf Channel (Fig. 10), respectively, which are similar to the values indicated by Ekau et al. (2010) for zooplankton. Our results also showed that macrozooplankton preferred oceanic waters with salinity values >31 g/kg, and temperatures between 8 and 10° C (Fig. 4, Fig. 9 and Fig. 10). Nonetheless, it must be considered that these preference values were estimated from observational data and limited sampling rather than from controlled experiments.

Vertical overlapping observed between fish and macrozooplankton abundances suggests that the prey-predator interactions might be enhanced under hypoxic conditions. Pollution and climate change are continually expanding the extent of hypoxic waters around the world, both in coastal waters and open oceans (Breitburg et al., 2018). While the links between recent anthropogenic perturbations, such as the salmon aquaculture expansion, and hypoxia in the Patagonian Fjords is still under debate, it is important to keep this potential impact upon habitat reductions and enhanced prey-predator interactions under consideration

as it might cause changes in zooplankton groups' distributions and abundance, particularly those that do not tolerate low DO concentrations.

The fact that some biological backscattering occurred within the hypoxic layer in our study indicates that hypoxia does not affect all macrozooplankton species equally and that some of them can inhabit this deeper layer, e.g., euphausiids species (Mass et al., 2014; Seibel et al., 2016). Hypoxia tolerant species residing below and within minimum DO layers have been reported, in fact, further north along the Chilean coast during the upwelling season, leading to support hypotheses on predation evasion and horizontal transport aimed to explain such behavior (Castro et al., 2007). Within this context *Euphausia pacifica* has been reported to exhibit the highest abundance of zooplankton species present in hypoxic waters in Hood Canal, Washington (Sato et al., 2016). Other euphausiids have also been reported to be present in other hypoxic systems in Chile (Escribano et al, 2009; Gonzalez et al., 2016). It has been shown that *Euphasia vallentini* is a dominant euphausiid species known to carry out extensive vertical migrations in Patagonian fjords, hence we speculate it might be one of the species occurring in the less oxygenated waters of our study. Unfortunately, due to sampling gear restrictions, we were unable to sample the hypoxic layer, nor to identify firmly the species occurring at this depth. Therefore, future research will be necessary to understand the relationship of the deep, yet scarce, macrozooplankton within the hypoxic waters in Puyuhuapi Fjord. As vertical mixing is a mechanism that could reduce the presence of hypoxic zones in fjords, values of TKE dissipation were compared to the depth strata of macrozooplankton.

5.3 Turbulent mixing at the fjord sill

Patagonian fjords and channels cover an area of ~240,000 km^2 and feature a complex marine topography, including submarine sills and channel constrictions (Pantoja et al., 2014; Inall and Gillibrand, 2010). Bernoulli aspiration, internal hydraulic jumps and intense tidal mixing are all processes that can be found near a fjord sill (Farmer and Freeland, 1983; Klymark and Gregg, 2003; Inall and Gillibrand, 2010; Whitney et al., 2014). Our data showed elevated values of TKE dissipation in Jacaf Channel ($\varepsilon = 10^{-5}$ W kg^{-1} and $K_\rho = 10^{-3}$ m^2 s^{-1}) near the sill from 0-60 m depth. These values are similar to those observed at the sill of Knight Inlet in Canada (Klymark and Gregg, 2003). Lower ε values were found in Puyuhuapi Fjord (Fig.11). The elevated vertical mixing (high K_ρ) in Jacaf Channel is probably due to the barotropic tide

interacting with the submarine sill (Schneider et al., 2014; Fig. 11, Fig.13 and Table 2). This was also observed in Martinez Channel (Pérez-Santos et al., 2014), Central Patagonia, where semidiurnal internal tides were found to dominate the estuarine dynamics (Ross et al., 2014). This region is highly influenced by the Baker river, whose discharge enhances stratification and introduces suspended solids that subsequently limit productivity in the water column (González et al., 2010; Daneri et al., 2012; González et al., 2013).

The evident aggregation of macrozooplankton and fish found near Jacaf sill (within ~1 km) matches the area exhibiting the highest ε values (~10^{-5} W kg^{-1}; Fig.13). Thin (2-5 m) and thick (10-50 m) regions of enhanced vertical shear measured directly with the VMP-250 microstructure profiler contribute to vertical mixing. Subsequently this enhances the exchange between the subsurface rich nutrient layer (Fig. 2) and the photic layer, leading to increased phytoplankton productivity (Montero et al., 2017a; Montero et al., 2017b), as shown in the conceptual model of figure 14. Thus, the acoustic and turbulence measurements collected near Jacaf sill promote the importance of a sill in influencing the vertical distribution of oxygen, macrozooplankton and fish on both sides of the sill.

A summary of the processes that can contribute to macrozooplankton vertical distribution and aggregation in Puyuhuapi Fjord and Jacaf Channel are presented in a Fig. 14. In Puyuhuapi Fjord, at 100 m depth a high nutrient and high production layer (Daneri et al., 2012; Montero et al., 2017a; Montero et al., 2017b) is separated from a hypoxic layer below, which limits species distribution and lacks significant aggregations of zooplankton. Above the hypoxic waters, turbulent mixing enhances contact between macrozooplankton predators and their prey (Visser et al., 2009). In Jacaf Channel, the hypoxic layer occurs deeper in the water column than in Puyuhuapi Fjord, which stretches the vertical distribution of macrozooplankton to a deeper range. Turbulent mixing also increases primary and secondary production, through enhanced nutrient availability and favors encounters of macrozooplankton with potential prey, increasing growth and survival rates (Visser and Stips 2002; MacCready et al., 2002; Klymak and Gregg 2004; Lee et al., 2005; Visser et al., 2009; Whitney et al., 2014).

5.4 Other findings and considerations

Results showed similar groups of macrozooplankton (>5 mm) in Puyuhuapi Fjord and Jacaf Channel: euphausiids, chaetognaths, medusae and siphonophores during summer

(January 2014) and winter (winter 2014). However, euphausiids were not observed in fall 2013, which was an unexpected result which deserves further confirmation and analysis. In contrast, fall 2013 sampling presented the highest acoustic abundances within the time series (Fig. 3). The elevated accumulation of macrozooplankton species around the sill may impose a significant modification in the amount and quality of carbon exported to deeper waters in particular zones of the fjords. Future studies on carbon flux quantification in fjords should incorporate sill regions to test this hypothesis, in order to improve ocean pumping assessments in the context of climate change and variability.

6 Conclusions

This paper was aimed to determine how hypoxic conditions affect the vertical distribution of macrozooplankton in fjords and to assess how vertical mixing relates to abundances of macrozooplankton at fjord sills. Results showed that the hypoxic layer in Patagonian Fjords limits DVM and overall distribution of macrozooplankton to the upper ~100 m of the water column, reducing the habitat of these species. The hypoxic zones were found away from underwater sills or areas that would experience enhanced turbulence. When assessing the abundance of macrozooplankton in conjunction with TKE dissipation near a submarine sill it was found that elevated turbulence generated by the barotropic tide interacting with the sharp bathymetric feature enhanced vertical mixing, deepened the hypoxic layer and injected nutrients. In addition, macrozooplankton were found in higher densities and extended deeper in the water column around the submarine sills. This is thought to be due to an increase in primary production that would result from the effects of elevated vertical mixing.

Acknowledgment

The ADCP data was collected as part of the FONDECYT Grant 3120038 and 11140161 by Dr. Iván Pérez-Santos and the help of Dr. Wolfgang Schneider's research group. We thank Dr. Arnoldo Valle-Levinson for motivating the acoustic study of zooplankton in Chilean Patagonia. We also thank Dr. Luis Cubillos and Dr. Billy Ernst for providing the scientific echo-sounder and Cristian Parra and Hernán Rebolledo for administering the scientific echo-sounder sampling. COPAS Sur-Austral CONICYT PIA PFB31 financed part of the field work and Lauren Ross's trips to Patagonia. We thank Juan Ramón Velasquez and Oscar Pizarro research group for his assistance in the ADCP 1, 2 and 3 moorings and Adolfo Mesa, Aldo

761 Balba and Eduardo Escalona for conducting most of the zooplankton sampling. Giovanni
762 Daneri is funded by FONDECYT Grant 1131063.
763

764 **References**

765 Ariza A., Landeira J.M., Escánez A., Wienerroither R., Aguilar de Soto N., Røstad A.,
766 Kaartvedt S., Hernández-León S.: Vertical distribution, composition and migratory
767 patterns of acoustic scattering layers in the Canary Islands. J. Mar. Syst, Vol. 157,
768 2016
769 Ayón, P., Criales-Hernandez M.I., Schwamborn R., Hirche H.J.: Zooplankton research off
770 Peru: a review. Prog. Oceanogr. 79, 238–255, 2008.
771 Ballón, M.: Acoustic study of macrozooplankton off Peru: biomass estimation, spatial
772 patterns, impact of physical forcing and effect on forage fish distribution. These.
773 Universite Montpellier II, 205 pp, 2010.
774 Ballón, M., Bertrand A., Lebourges-Dhaussy A., Gutiérrez M., Ayón P., Grados, D., Gerlotto
775 F.: Is there enough zooplankton to feed forage fish populations off Peru? An acoustic
776 (positive) answer. Prog. Oceanogr., 91(4): 360-381, 2011.
777 Basedow, S.L., Eliane, K., Tverberg, V., Spindler, M.: Advection of zooplankton in an Arctic
778 fjord (Kongsfjorden, Svalbard). Estuarine, Coastal and Shelf Science, 60(1), 113-124,
779 2004.Bearman, G.: Waves, tides and shallow water processes. Butterworth-
780 Heinemann, Oxford, 187 pp, 1989.
781 Berge J., Cottier F., Last K., Varpe Ø., Leu E., Søreide J., Eiane K., Falk-Petersen S., Willis
782 K., Nygård H., Vogedes D., Griffiths C., Johnsen G., Lorentzen D., Brierley A.: Diel
783 vertical migration of Arctic zooplankton during the polar night. Biol. Lett. 5 69-72,
784 2009.
785 Buchholz F., Buchholz C., Reppin J., Fischer J.: Diel vertical migrations of *Meganyctiphanes*
786 *norvegica* in the Kattegat: Comparison of net catches and measurements with Acoustic
787 Doppler Current Profilers. Helgolander Meeresunters, 49, 849-866, 1995.
788 Breitburg, D. et al.: Declining oxygen in the global ocean and coastal waters. Science 359, 1-
789 11, 2018.
790 Brierley A., Saunders R. A., Bone D. G., Murphy E. J., Enderlein P., Conti S. G., Demer D.
791 A.: Use of moored acoustic instruments to measure short-term variability in
792 abundance of Antarctic krill, Limnol. Oceanogr.: Methods 4,18–29, 2006.

Cade D. E. and Benoit-Bird K.J.: Depths, migration rates and environmental associations of acoustic scattering layers in the Gulf of California. Deep Sea Res. Part I: Oceanographic Research Papers, Vol. 102, Pages 78-89, 2015.

Castillo, M. I., Cifuentes, U., Pizarro, O., Djurfeldt, L., and Caceres, M.: Seasonal hydrography and surface outflow in a fjord with a deep sill: the Reloncaví fjord, Chile, Ocean Sci., 12, 533-544, https://doi.org/10.5194/os-12-533-2016, 2016.

Castro, L.R., Bernal, P.A., Troncoso, V.A.: Coastal intrusion of copepods: mechanisms and consequences in the population biology of *Rhincalanus nasutus*. J. Plankton Res. 15 (5), 501–515, 1993.

Castro L. R., Troncoso V. A.: Fine-scale vertical distribution of coastal and offshore copepods in the Golfo de Arauco, central Chile, during the upwelling season, Prog. Oceanogr. 75(3): 486-500, 2007.

Castro L.R., M.A. Caceres, N. Silva, M.I. Muñoz, R. León, M.F. Landaeta, Soto Mendoza S.: Short-term variations in mesozooplankton, ichthyoplankton, and nutrients associated with semi-diurnal tides in a Patagonian Gulf, Con. Shelf Res., Vol. 31, 3–4, 282–292, 2014.

Cloern, J.: Tidal stirring and phytoplankton bloom dynamics in an estuary, J. Mar. Res., 49, 203-221.

Daneri, G., Montero P., Lizárraga L., Torres R., Iriarte J.L., Jacob B., González H.E. and Tapia F.J.: Primary productivity and heterotrophic activity in an enclosed marine area of central Patagonia (Puyuhuapi channel; 44S, 73W). Biogeosciences Discuss 9, 5929–5968, 2012.

Díaz, R. J.: Overview of hypoxia around the world, J. Environ.Qual., 30, 275–281, 2001

Díaz-Astudillo M., Cáceres M, Landaeta M.: Zooplankton structure and vertical migration: Using acoustics and biomass to compare stratified and mixed fjord systems. Cont. Shelf Res., 148, 208-218, 2017.

Dyer, K.R.: Estuaries: A physical introduction. John Wiley & Sons, West Sussex, England, 1997.Ekau W., Auel H., Portner H.-O. and Gilbert D.: Impacts of hypoxia on the structure and processes in pelagic communities (zooplankton, macro-invertebrates and fish). Biogeosciences, 7, 1669–1699, 2010.

824 Escribano R., Hidalgo P., Krautz C.: Zooplankton associated with the oxygen minimum zone
825 system in the northern upwelling region of Chile during March 2000. Deep Sea
826 Research Part II: Topical Studies in Oceanography, 56, Issue 16, 1083-1094, 2009.
827 Farmer, D. M. and Freeland, H. J.: The physical oceanography of fjords, Prog. Oceanogr., 12,
828 147–194, 1983.
829 Fielding, S., Griffiths, G., and Roe, H. S. J.: The biological validation of ADCP acoustic
830 backscatter through direct comparison with net samples and model predictions based
831 on acoustic-scattering models. J of Marine Science, 61,184-200, 2004.Foreman,
832 M.G.G.: Manual for Tidal Heights Analysis and Prediction. Pacific Marine Science
833 Report 77-10, 1977.
834 Foreman, M.G.G.: Manual for Tidal Currents Analysis and Prediction. Pacific Marine Science
835 Report 78-6, 1978.
836 Foote K.G, Knudsen H.P., Vestnes G., MacLennan D.N., Simmonds E.J.: Calibration of
837 acoustic instruments for fish density estimation: a practical guide. ICES cooperative
838 research report N° 144. International Council for the Exploration of the Sea,
839 Copenhaguen, Denmark, 1987.
840 Fuenzalida, R., Schneider, W., Garcés-Vargas, J., Bravo, L., Lange, C.: Vertical and
841 horizontal extension of the oxygen mínimum zone in the eastern South Pacific Ocean.
842 Deep-Sea Research II, 56, 1027–1038, 2009.Gagnon, M., Lacroix, G.: The effects of
843 tidal advection and mixing on the statistical dispersion of zooplankton, J. Exp. Mar.
844 Biol. Ecol., 56, 9—22, 1982.
845 Gattuso. J., Frankingnoulle M., Wollast R.: Carbon and carbonate metabolism in coastal
846 aquatic ecosystems, Annu. Rev. Ecol. Syst. 29: 405-434, 1998.
847 Giesecke, R., González, H.E.: Feeding of *Sagitta enflata* and vertical distribution of
848 chaetognaths in relation to low oxygen concentrations. J. Plankton Res 26, 475-486,
849 2005.
850 González, H. E., Calderon, M. J., Castro, L., Clement, A., Cuevas, L. A., Daneri, G., Iriarte, J.
851 30 L., Lizárraga, L., Martinez, R., Menschel, E., Silva, N., Carrasco, C., Valenzuela,
852 C., Vargas, C. A., and Molinet, C.: Primary Production and plankton dynamics in the
853 Reloncavi Fjord and the Interior Sea of Chiloe, Northern Patagonia, Chile, Mar. Ecol.
854 Prog. Ser., 402, 13–30, 2010.

González, H. E., Castro L., Daneri G., Iriarte J.L., Silva N., Vargas C., Giesecke R., Sánchez N.: Seasonal plankton variability in Chilean Patagonia Fjords: carbon flow through the pelagic foodweb of the Aysen Fjord and plankton dynamics in the Moraleda Channel basin, Cont Shelf Res 31,225-243, 2011.

González H. E., Castro L.R., Daneri G., Iriarte J.L., Silva N., Tapia F., Teca E. and Vargas C.A.: Land-ocean gradient in haline stratification and its effects on plankton dynamics and trophic carbon fluxes in Chilean Patagonian fjords (47° – 50°S), Prog. Oceanogr. 119: 32-47, 2013.

González H. E, M. Graeve, G. Kattner, N. Silva, L. Castro, J. L. Iriarte, L. Osmán, G. Daneri, Vargas C. A.: Carbon flow through the pelagic food web in southern Chilean Patagonia: relevance of *Euphausia vallentini* as key species. Marine Ecology Progress Series 557:91-110, 2016.

Godin, G.: The Analysis of Tides. University of Toronto Press, Toronto, 1972

Godin, G.: Tides. ANADYOMENE Edition, Ottaea, Notario, 1988.

Govani, J.J., Hoss, D.E., Colby, D.R.: The spatial distribution of larval fishes about the Mississippi River plume, Limnol. Oceanogr., 34, 178-187, 1989.Greene C.H. and Peter H.W.: Bioacoustical oceanography: New tools for zooplankton and micronekton research in the 1990s, Oceanography, 3, 12-17, 1990.

Van Haren H. and Compton T.J.: Diel Vertical Migration in Deep Sea Plankton Is Finely Tuned to Latitudinal and Seasonal Day Length. PLoS ONE 8(5): e64435. doi:10.1371/journal.pone.0064435, 2013.

Haury, L.R., Yamazaki H., Itsweire E.C.: Effects of turbulent shear flow on zooplankton distribution, Deep-sea Res, 37(3), 447—461, 1990.

Hauss, H., Christiansen, S., Schütte, F., Kiko, R., Edvam Lima, M., Rodrigues, E., Karstensen, J., Löscher, C. R., Körtzinger, A., and Fiedler, B.: Dead zone or oasis in the open ocean? Zooplankton distribution and migration in low-oxygen modewater eddies, Biogeosciences, 13, 1977-1989, https://doi.org/10.5194/bg-13-1977-2016, 2016.

Heywood, K.: Diel vertical migration of zooplankton in theNortheast Atlantic. J Plankton Res. 18-2, 163-184, 1996.Horne, J.K., Jech J.M.: Multi-frequency estimates of fish abundance: constraints of rather high frequencies. J Marine Sci. 56, 184–199, 1999.

Holliday, D.V. and Pieper R.E.: Bioacoustical oceanography at high frequencies. J. Marine Sci. 52, 279–296, 1995.

Inall, M. E. and Gillibrand, P. A.: The physics of mid-latitude fjords: a review, Geological Society, London, UK, Special Publications 344, 17–33, 2010.

Klevjer, T. A., Irigoien X., Røstad A., Fraile-Nuez E., Benítez-Barrios V. M. and Kaartvedt S.: Large scale patterns in vertical distribution and behaviour of mesopelagic scattering layers. *Sci. Rep.* 6, 19873; 2016.

Kloser, R.J., Ryan T., Sakov P., Willliams A., Koslow J.A.: Species identification in deep water using multiple acoustic frequencies. Canadian Journal of Fisheries and Aquatic Sciences 59, 1065–1077, 2016

klymak, J., and Gregg M.: Tidally generated turbulence over the Knight Inlet sill, J. Phys. Oceanogr., 34, 1135-1151, 2003.

Koseff, J., Holen, J., Monismith, S., Cloern, J.: Coupled effects of vertical mixing and benthic grazing on phytoplankton populations in shallow, turbid estuaries, J. Mar. Res., 51, 843-868, 1993.Landaeta M., Martínez R., Bustos C. and Castro L.: Distribution of microplankton and fish larvae related to sharp clines in a Patagonian fjord. Revista de Biología Marina y Oceanografía, Vol. 48, Nº2: 401-407, 2013.

Lee, K., Mukai T., Kang D., Iida K.: Application of acoustic Doppler current profiler combined with a scientific echo-sounder for krill Euphausia pacifica density estimation, Fisheries Science, 70: 1051–1060, 2004.

Lee K., Mukai T., Lee D., Iida K.: Verification of mean volume backscattering strength obtained from acoustic Doppler current profiler by using sound scattering layer, Fisheries Science, 74: 221–229, 2008.

Lee, O., Nash, R.D.M., Danilowicz, B.S.: Small-scale spatio-temporal variability in ichthyoplankton and zooplankton distribution in relation to a tidal-mixing front in the Irish Sea, J. Mar. Sci., 62, 1021—1036, 2005, doi:10.1016/j.icesjms.2005.04.016.

Lewis, D., and Pedley, T.: The Infuence of Turbulence on Plankton Predation Strategies, J. theor. Biol. 210, 347-365, 2001.

Logerwell, E.A., Wilson C.: Species discrimination of fish using frequencydependent acoustic backscatter. J Marine Sci., 61, 1004–1013, 2004.

Lough, R.G., Manning, J.P.: Tidal-front entrainment and retention of fish larvae on the southern flank of Georges Bank, Deep Sea Research, 48 Suppl. 2, 631-644, 2001.

MacCready, P., Hetland, R., Geyer, R.: Long-term isohaline salt balance in an estuary, Cont. Shelf. Res., 22, 1591-1601, 2002.

Maas, A.M., Frazar, S.L., Outram, D.M., Seibel, B.A., Wishner, K.F.: Fine-scale vertical distribution of macroplankton andmicronekton in the Eastern Tropical North Pacific inassociation with an oxygen minimum zone, J. Plankton Res. 36-6,1557–1575, 2014.

Mair A., Fernandes P., Lebourges-Dhaussy A and Brierley A.: An investigation into the zooplankton composition of a prominent 38-khz scattering layer in the North Sea. J. Plank. Res. 27, 7, 623-633, 2005.

Meerhoff, E., Castro L.and Tapia F.: Influence of freshwater discharges and tides on the abundance and distribution of larval and juvenile Munida gregaria in then Baker river estuary, Chilean Patagonia, Cont. Shelf. Res. 61–62, 1–11, 2013.

Meerhoff, E., Tapia, F.J., Sobarzo, M., Castro, L.: Influence of estuarine and secondary circulation on crustacean larval fluxes: a case study from a Patagonian fjord., J. Plankton Res. 37(1), 168—182, 2015. Doi:10.2093/plankt/fbu106.

Montero, P., Pérez-Santos I., Daneri G., Gutiérrez M., Igor G., Seguel R., Crawford D., Duncan P.: A winter dinoflagellate bloom drives high rates of primary production in a Patagonian fjord ecosystem, Estuar. Coast. Shelf Sci., 199, 105-116, 2017a.

Montero P, Daneri G., Tapia F., Iriarte JL. and Crawford D.: Diatom blooms and primary production in a channel ecosystem of central Patagonia. Lat. Am. J. Aquat. Res., 45,(5), 999-1016, 2017b.

Mosteiro, A., Fernandes P.G., Armstrong F., Greenstreet S.P.R.: A Dual Frequency Algorithm for the Identification of Sandeel School Echotraces. ICES Document CM 2004/R: 12, 13pp, 2004.

Munk, P., Wright, P.J., Pihl, N.J.: Distribution of the early larval stages of Cod, Plaice and Lesser Sandeel across haline fronts in the North Sea. Estuarine, Coastal and Shelf Science, 55(1), 139-149, 2002.

Murase, H., Ichihara M., Yasuma H., Watanabe H., Yonezaki S., Nagashima H., Kawahara S., Miyashita K.: Acoustic characterization of biological backscatterings in the

948 Kuroshio–Oyashio inter-frontal zone and subarctic waters of the western North Pacific
949 in spring. Fis. Oceanogr. 18,386–401, 2009.
950 North E.W., Houde E.D.: Retention of white perch and striped bass larvae: biological-
951 physical interactions in Chesapeake Bay estuarine turbidity maximum. Estuaries
952 24:756–769,2001.
953 North E.W., Houde E.D.: Distribution and transport of bay anchovy (Anchoa mitchilli) eggs
954 and larvae in Chesapeake Bay. Estuarine, Coastal and Shelf Science 60:409–429,
955 2004.
956 North E.W., Schlag Z., Hood R.R., Li M., Zhong L., Gross T., Kennedy V.S.: Vertical
957 swimming behavior influences the dispersal of simulated oyster larvae in a coupled
958 particle-tracking and hydrodynamic model of Chesapeake Bay. Marine Ecology
959 Progress Series 359:99–115, 2008.
960 Oviatt, C.A.: Effects of different mixing schedules on phytoplankton, zooplankton and
961 nutrients in marine microcosms, Mar. Ecol. Prog. Ser., 4, 57—67, 1981.
962 Pagés, F., González H.E., Ramon, M., Sobarzo, M., Gili, J.M.: Gelatinous zooplankton
963 assemblages associated with wáter masses in the Humboldt Current System, and
964 potential predatory impact by *Bassia bassensis* (Siphonophora; Calycophorae). Mar.
965 Ecol. Prog. Ser., 210, 13-24, 2001.
966 Palma S.: Zooplankton distribution and abundance in the austral Chilean channels and fjords.
967 Progress in the oceanographic knowledge of Chilean inner waters, from Puerto Montt
968 to Cape Horn. Comité Oceanográfico Nacional - Pontificia Universidad Católica de
969 Valparaíso, Valparaíso, Chile, pp. 107-113. Book on line at http://www.cona.cl/, 2008.
970 Paulmier, A. and Ruiz-Pino, D.: Oxygen minimum zones (OMZs) in the modern ocean.
971 Progress in Oceanography, 80, 113–128, 2009.Pawlowicz, R., Beardsley B., and Lentz
972 S.: "Classical tidal harmonic analysis including error estimates in MATLAB using
973 T_TIDE", Computers and Geosciences 28, 929-937, 2002.
974 Pantoja, S., Iriarte L., and Daneri, G.: Oceanography of the Chilean Patagonia, Cont. Shelf
975 Res., 31, 149–153, 2011.
976 Pérez-Santos I., Garcés-Vargas J., Schneider W., Ross L., Parra S., Valle-Levinson A.:
977 Double-diffusive layering and mixing in Patagonia fjords, Prog. Oceanogr., 129, 35-
978 49, 2014.

Pérez-Santos, I.: Deep ventilation event during fall and winter of 2015 in Puyuhuapi fjord (44.6°S). Lajar, 45(1), 223-225, 2017.

Peters, H., Bokhorst, R.: Microstructure observations of turbulent mixing in a partially mixed estuary. Part II: Salt flux and stress, J. Phys. Oceanogr., 31, 1105-1119, 2001.

Ressler, P.H.: Acoustic backscatter measurements with a 153 kHz ADCP in the northeastern Gulf of Mexico: determination of dominant zooplankton and micronekton scatterers, Deep Sea Research Part I: Oceanographic Research Papers 49 (11), 2035-2051, 2002.

Rodriguez, J.M., Hernandez-Leon, S., Barton, E.D.: Mesoscale distribution of fish larvae in relation to an upwelling filament off northwest Africa, Deep Sea Research I, 46, 1969-1984, 1999.

Robinson, C., and Gómez-Gutiérrez J.: Daily vertical migration of dense deep scattering layers to the shelf-break along the northwest coast of Baja California, Mexico. J. Plankton Res. 20-9, 1679-1697,1998.

Ross, L., Pérez-Santos I., Valle-levinson A., Schneider W.: Semidiurnal internal tides in a Patagonian fjord, Prog. Oceanogr., 129, Part A, 19-34, 2014.

Røstad, A. and Kaartvedt S.: Seasonal and diel patterns in sedimentary flux of krill fecal pellets recorded by an echo-sounder 1,2 Limnol. Oceanogr., 58 (6), 1985–1997,2013.

Sato, M.: Variability in Diel Vertical Migration of Zooplankton and Physical Properties in Saanich Inlet, British Columbia. A Dissertation Submitted in Partial Fulfillment of the Requirements for the Degree of DOCTOR OF PHILOSOPHY in the School of Earth and Ocean Sciences. University of Victoria, 2013.

Sato, M., Horne J., Parker-Stetter S., Essington T., Keister J., Moriarty P., Li L., Newton J.: Impacts of moderate hypoxia on fish and zooplankton prey distributions in a coastal fjord. Mar. Ecol. Prog. Ser, Vol. 560: 57–72, 2016.

Seibel, B.A., Schneider, J.L., Kaartvedt, S., Wishner, K.F., Daly, K.L.: Hypoxia Tolerance and Metabolic Suppression in Oxygen Minimum Zone Euphausiids: Implications for Ocean Deoxygenation and Biogeochemical Cycles. Integrative and Comparative Biology,56-4, 510–523, 2016.Silva, N. and Vargas, C.: Hypoxia in Chilean Patagonia fjords, Prog. Oceanogr., 129, 62-74, 2014.

Sievers, A.H. and Silva, N.: Water masses and circulation in austral Chilean channels and fjords, in: Silva, N., Palma, S. (Eds.), Progress in the oceanographic knowledge of Chilean inner waters, from Puerto Montt to Cape Horn. Comité Oceanográfico

Nacional - Pontificia Universidad Católica de Valparaíso, Valparaíso, Chile, pp. 53-58. Book on line at http://www.cona.cl/, 2008.

Simmonds EJ, MacLennan D.N.: Fisheries Acoustics: Theory and Practice, 2nd edn. London: Blackwell Science; 437 p, 2005.

Schneider, W., Pérez-Santos I., Ross L., Bravo L., Seguel R., Hernández F.: On the hydrography of Puyuhuapi Channel, Chilean Patagonia, Prog. Oceanogr., 128, 8-18, 2014.

Strickland, J.D.H. and Parsons, T.R.: A Practical Handbook of Seawater Analysis. Bull. Fish. Res. Board Can. 167, 1968

Valle-Levinson A., Castro L., Cáceres M., Pizarro O.: Twilight vertical migrations of zooplankton in a Chilean fjord, Prog. Oceanogr. 129, 114-124, 2014.

Visser A. and Stips A.: Turbulence and zooplankton production: insights from PROVESS. J. Sea Res 47, 317– 329, 2002.

Visser, A., Mariani P., Pigolotti S.: Swimming in turbulence: zooplankton fitness in terms of foraging efficiency and predation risk, J Plankton Res., 31 (2): 121-133, 2009.

Whitney M., Jia Y., Pearse M., Christopher J. K.: Sill effects on physical dynamics in eastern Long Island Sound. Ocean Dynamics, 64:443–458, 2017.Zhou M., Dorland R. Aggregation and verticalmigration behavior of *Euphausia superba*. Deep-Sea Res. II 51, 2119–2137, 2004.

Figure captions

Figure 1. Study area in relation to South America and the Pacific Ocean is the small panel in the top right. The main figure enlarges the study area (Puyuhuapi Fjord and Jacaf Channel) and indicates the instruments used for data collection, fixed point station positions, and the sill location near the head of Jacaf Channel. The contours indicate the depth of the fjords.

Figure 2. (Upper panel) Profiles of temperature (a-b), salinity (c-d), dissolved oxygen (e-f) and nitrate (g) collected during different oceanographic campaigns in the northern central part of Puyuhuapi Fjord and (lower panel) in eastern region of the Jacaf Channel.

Figure 3. (a) Volume backscattering strength (S_v,) calculated from the ADCP-1 backscatter signal in Puyuhuapi Fjord, deployed at 50 m depth from the 8th to the 26th of May, 2013. (b) Zoom of the S_v data and the times of *in-situ* zooplankton sampling (black dots) carried out during May 25-26, 2013. (c-d) Vertical abundance of main zooplankton groups (>5 mm length) from the *in-situ* sampling at 16:00 and 18:00 (local time) on May 25th and (e-f) at 9:00 and 11:00 (local time) on May 26th.

Figure 4. (a) Volume backscattering strength (S_v) calculated from the ADCP-2 backscatter signal in Puyuhuapi Fjord from the 22nd to the 24th of January, 2014. The *in-situ* zooplankton sampling (in 3:00 intervals) are represented by black dots at the surface. (b) Depth integrated abundance of zooplankton from the surface to 100 m depth varying throughout time, where the top panel is zooplankton > 5 mm in length. (c) Vertical abundance of the principal zooplanktons groups on January 23rd at 2:00 (night time) and (d, e and f) same as (c) but on January 23rd at 08:00 and 14:00 (daytime) and January 24th at 02:00 (night time). The time reference is in local time.

Figure 5. Single frequency (38 kHz) scientific echo-sounder transect conducted along the Puyuhuapi Fjord during the Summertime field campaign (January 2014). Distribution indicated by colors representing S_v. (a) Daytime transect of echo-sounder measurements (S_v) throughout depth (*y*-axis) from the mouth (0 km) to the head (80 km) of Puyuhuapi Fjord on January 22, 2014. (b) Average profiles derived from the Nautical Area Scattering Coefficient (NASC) from the daytime transect with standard deviation bars, (c) Same as (a), but for the night time starting at 21:57 (local time) January 24th through early in the morning of January 25, 2014. (d) Same as (b) but for the nighttime. The ADCP-2 mooring location is marked with a black dot in (a) and (c). (e) Dissolved oxygen profiles (black dots) obtained approximately

every three hours (close to the position of ADCP-2 mooring) from January 23rd to 24th, 2014. The location of the hypoxic boundary layer is depicted by the white contour line of 2 mL L^{-1}.

Figure 6. Scatter plot of volume backscattering strength (S_v) from 38 kHz frequency and the most abundance macrozooplankton species obtained in the *in-situ* fixed stations carried out in Puyuhuapi Fjord (a, b and c) during January 22-24, 2014 and (d, e) in Jacaf Channel during August 18-19, 2014.

Figure 7. Dual-frequency (38 and 120 kHz) scientific echo-sounder transects along Puyuhuapi Fjord (0-18 km) and Jacaf Channel (18-35 km) during nighttime on August 17, 2014. (a) Fluid like and (b) blue noise echogram for zooplankton and (c) the fish echogram. Distribution indicated by colors representing *Sv* values. The black arrow in (a) represents the entrance to Jacaf Channel. Horizontal red lines in (a, b, c) denote lower limits of usable acoustic data (250 m).

Figure 8. Dual-frequency (38 and 120 kHz) acoustic transect across Jacaf sill conducted during daytime on August 18, 2014. (a) Fluid-like echogram, (b) blue noise echogram for zooplankton and (c) the fish echogram. Distribution indicated by colors representing S_v values. Horizontal red lines in (a, b, c) denote lower limits of usable acoustic data (250 m).

Figure 9. (a-d) *In-situ* stratified zooplankton sampling along Jacaf Channel during August 17, 2014 and the acoustic data collected simultaneously using the dual-frequency (38 and 120 kHz). FL is fluid-like and BN is blue noise groups. (e) Depth integrated abundance of macrozooplankton groups from surface to 150 m depth for various sampling hours. (f) Showed the stations positions. (g-j) The vertical abundance of the main macrozooplankton groups found during the wintertime survey.

Figure 10. Relationships between the relative abundance of zooplankton (expressed in S_v values) using 38 kHz frequency echo-sounder measurements (*y*-axis) and temperature in (a) Puyhuhuapi Fjord and (b) Jacaf Channel; salinity in (c) Puyuhuapi Fjord and (d) Jacaf Channel; dissolved oxygen in (e) Puyuhuapi Fjord and (f) Jacaf Channel; oxygen saturation in (g) from Puyuhuapi Fjord and (bh) Jacaf Channel. The black lines denote the quadratic fit curves, contour colors indicate depth.

Figure 11. Profiles of water temperature (blue line), vertical shear (red line) and dissipation rate of turbulent kinetic energy (black line with green dots) obtained with the VMP-250 microprofiler at the depth of the Jacaf sill (~140 m depth) in (a) Jacaf Channel on 21 November 2013 (c) Puyuhuapi Fjord on 22 November 2013 and (e) in Puyuhuapi Fjord on 23

January 2014. (b, d, f) Reprentative spectrum of velocity shear ($\partial u/\partial z$) for shear probe 1 (blue line) and 2 (red line) in wavenumber space in Jacaf Channel on 21 November 2013, Puyuhuapi Fjord on 22 November 2013 and Puyuhuapi Fjord on 23 January 2014, respectively. The black line denotes the dimensional Nasmyth spectrum and the red and blue triangles the cut-off of maximum wavenumber (k_{max}) for each shear probe. The shear spectrums were carried out in the same layer (135-145 m) for all turbulence profilers.

Figure 12. Scatter plot of dissipation rate of turbulent kinetic energy (ε) and (a) volume backscattering strength (S_v) from 38 kHz frequency and (b, c and d) the most abundance macrozooplankton species obtained in the *in-situ* fixed stations carried out in Puyuhuapi Fjord during Junuary 22-24, 2014.

Figure 13. (a) Microstructure profile locations along Jacaf Channel and sill using VMP-250 in November 2013. (b) The color bar showed the dissipation rate of turbulent kinetic energy (ε) and the blue lines depict the velocity shear at each station location along Jacaf Channel (as shown in (a). The horizontal scale (-2 to 2 s^{-1}) applied to profiles at stations 160, 162 and 163. Station 164 is located at the confluence of Jacaf Channel and Puyuhuapi Fjord (10.5 km) (c) The diapycnal eddy diffusivity profiles (K_p), obtained at each station shown in (a).

Figure 14. Conceptual model to show the oceanographic processes that contribute to the distribution and aggregation of zooplankton in (a) Puyuhuapi Fjord and (b) Jacaf Channel.

Table captions

Table 1. Data set collected during oceanographic campaigns in Puyuhuapi Fjord and Jacaf Channel.

Table 2. Harmonic analysis implemented to water level time series in Puyuhuapi Fjord and Jacaf Channel.

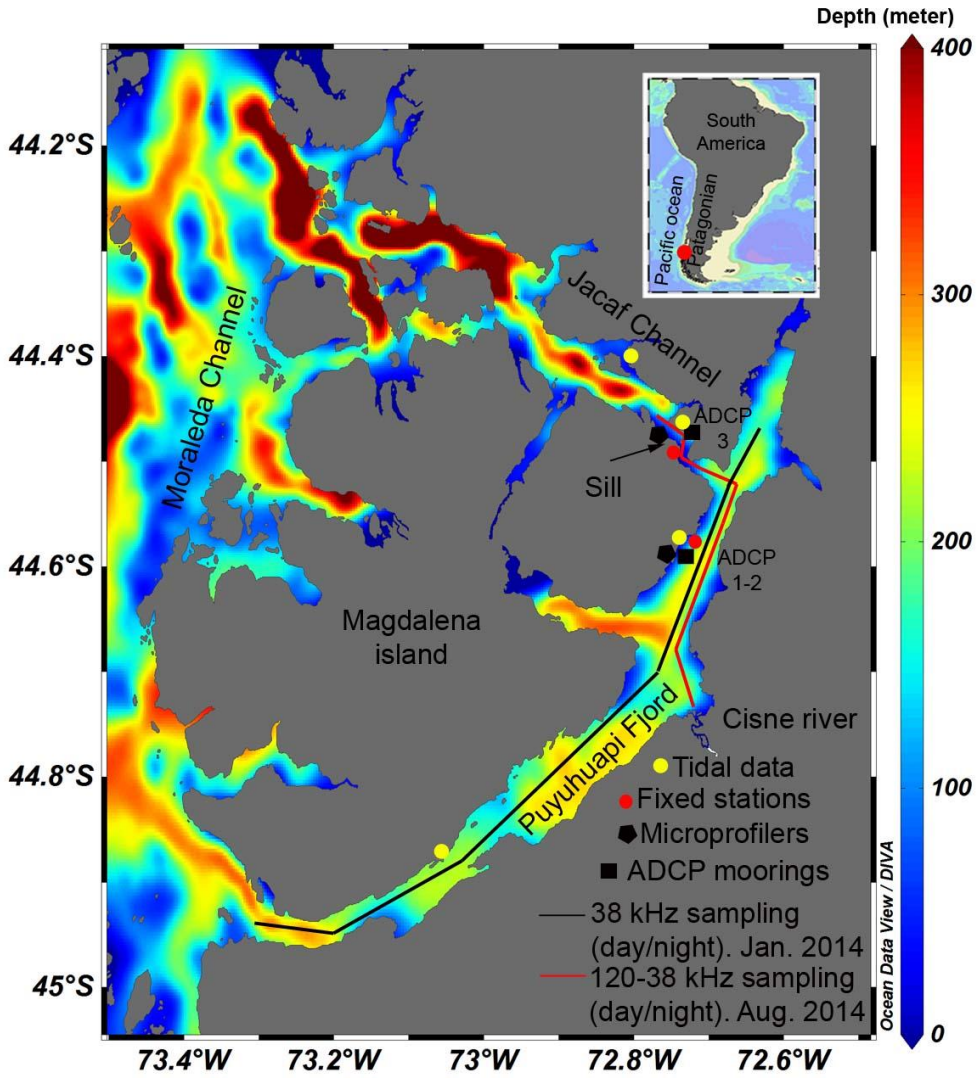

Figure 1. Study area in relation to South America and the Pacific Ocean is the small panel in the top right. The main figure enlarges the study area (Puyuhuapi Fjord and Jacaf Channel) and indicates the instruments used for data collection, fixed point station positions, and the sill location near the head of Jacaf Channel. The contours indicate the depth of the fjords.

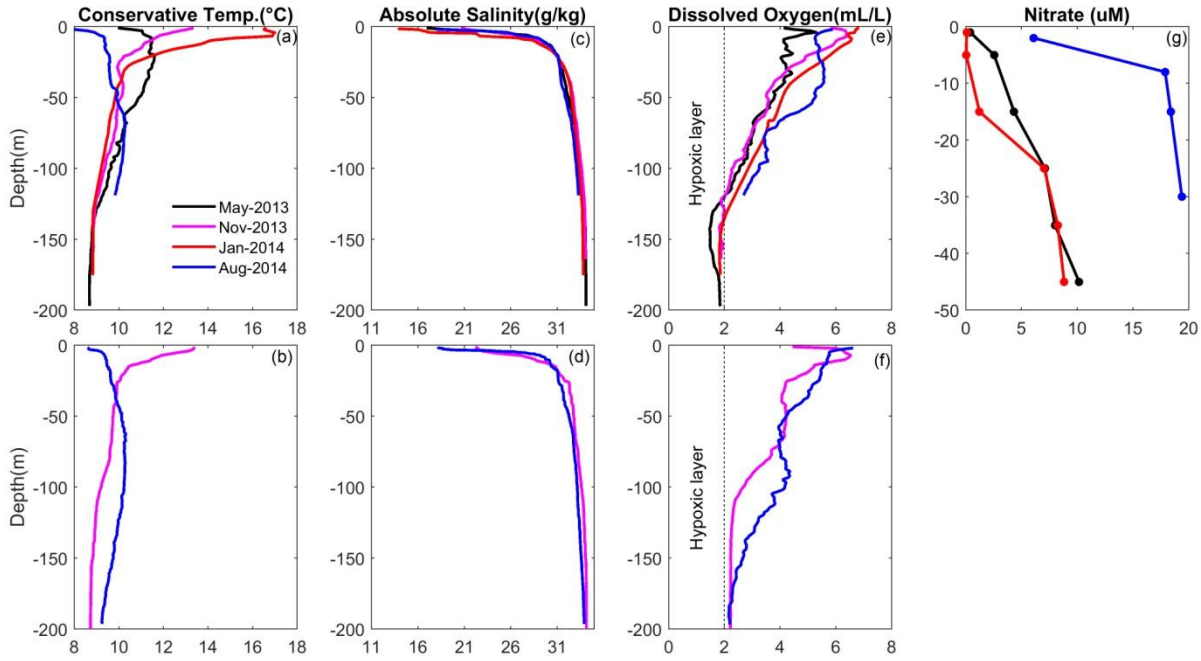

1126

1127 Figure 2. (Upper panel) Profiles of temperature (a-b), salinity (c-d), dissolved oxygen (e-f)
1128 and nitrate (g) collected during different oceanographic campaigns in the northern central part
1129 of Puyuhuapi Fjord and (lower panel) in eastern region of the Jacaf Channel.

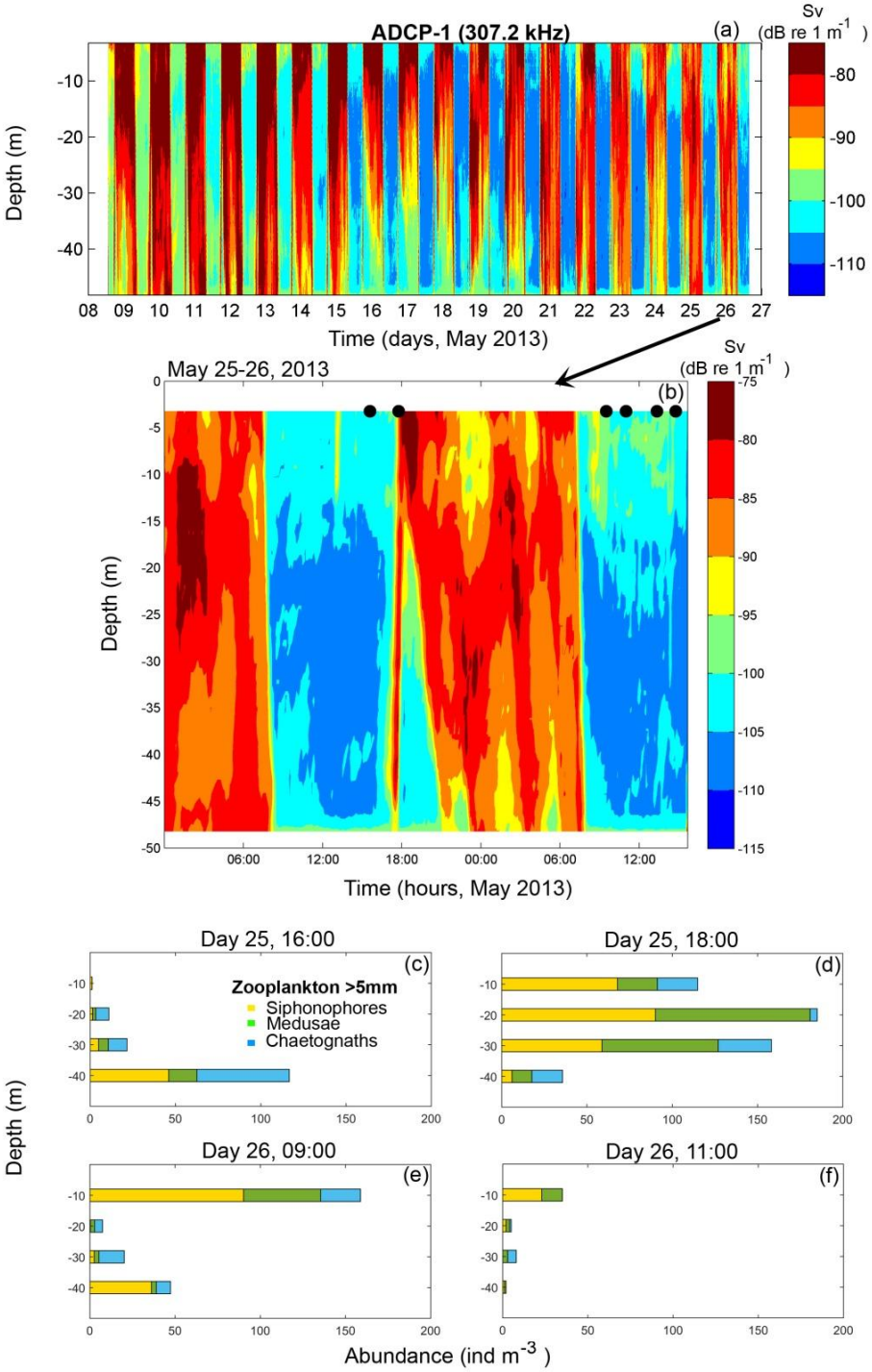

Figure 3. (a) Volume backscattering strength (S_v,) calculated from the ADCP-1 backscatter signal in Puyuhuapi Fjord, deployed at 50 m depth from the 8th to the 26th of May, 2013. (b) Zoom of the S_v data and the times of *in-situ* zooplankton sampling (black dots) carried out during May 25-26, 2013. (c-d) Vertical abundance of main zooplankton groups (>5 mm length) from the *in-situ* sampling at 16:00 and 18:00 (local time) on May 25th and (e-f) at 9:00 and 11:00 (local time) on May 26th.

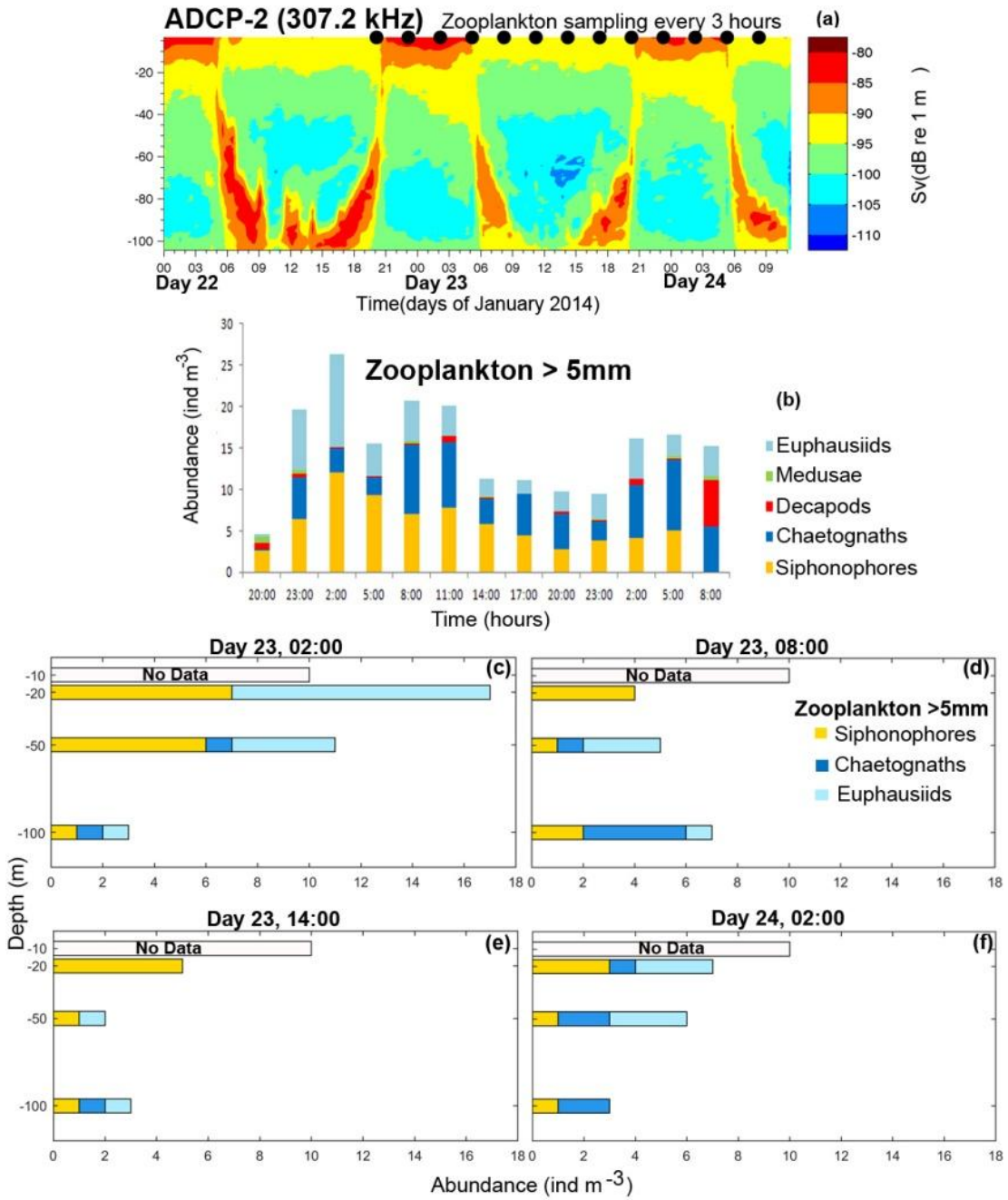

Figure 4. (a) Volume backscattering strength (S_v) calculated from the ADCP-2 backscatter signal in Puyuhuapi Fjord from the 22nd to the 24th of January, 2014. The *in-situ* zooplankton sampling (in 3:00 intervals) are represented by black dots at the surface. (b) Depth integrated abundance of zooplankton from the surface to 100 m depth varying throughout time, where the top panel is zooplankton > 5 mm in. (c) Vertical abundance of the principal zooplanktons groups on January 23rd at 2:00 (nighttime) and (d, e and f) same as (c) but on January 23rd at 8:00 and 14:00 (daytime) and January 24th at 02:00 (nighttime). The time reference is in local time.

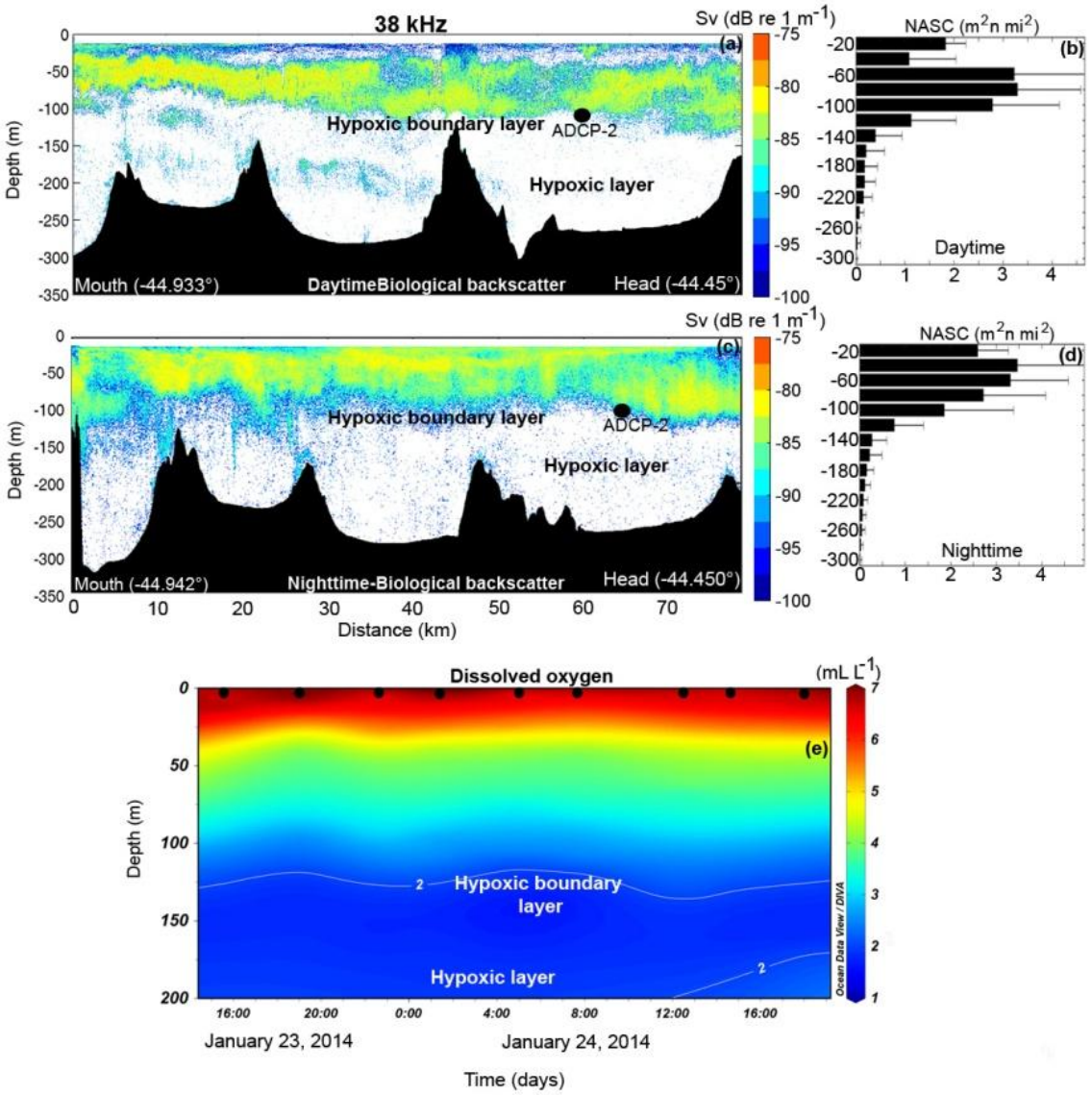

Figure 5. Single frequency (38 kHz) scientific echo-sounder transect conducted along the Puyuhuapi Fjord during the summertime field campaign (January 2014). Distribution indicated by colors representing S_v. (a) Daytime transect of echo-sounder measurements (S_v) throughout depth (y-axis) from the mouth (0 km) to the head (80 km) of Puyuhuapi Fjord on January 22, 2014. (b) Average profiles derived from the Nautical Area Scattering Coefficient (NASC) from the daytime transect with standard deviation bars. (c) Same as (a), but for the nighttime starting at 21:57 (local time) January 24th through early in the morning of January 25, 2014. (d) Same as (b) but for the nighttime. The ADCP-2 mooring location is marked with a black dot in (a) and (c). (e) Dissolved oxygen profiles (black dots) obtained approximately every three hours (close to the position of ADCP-2 mooring) from January 23rd to 24th, 2014. The location of the hypoxic boundary layer is depicted by the white contour line of 2 mL L^{-1}.

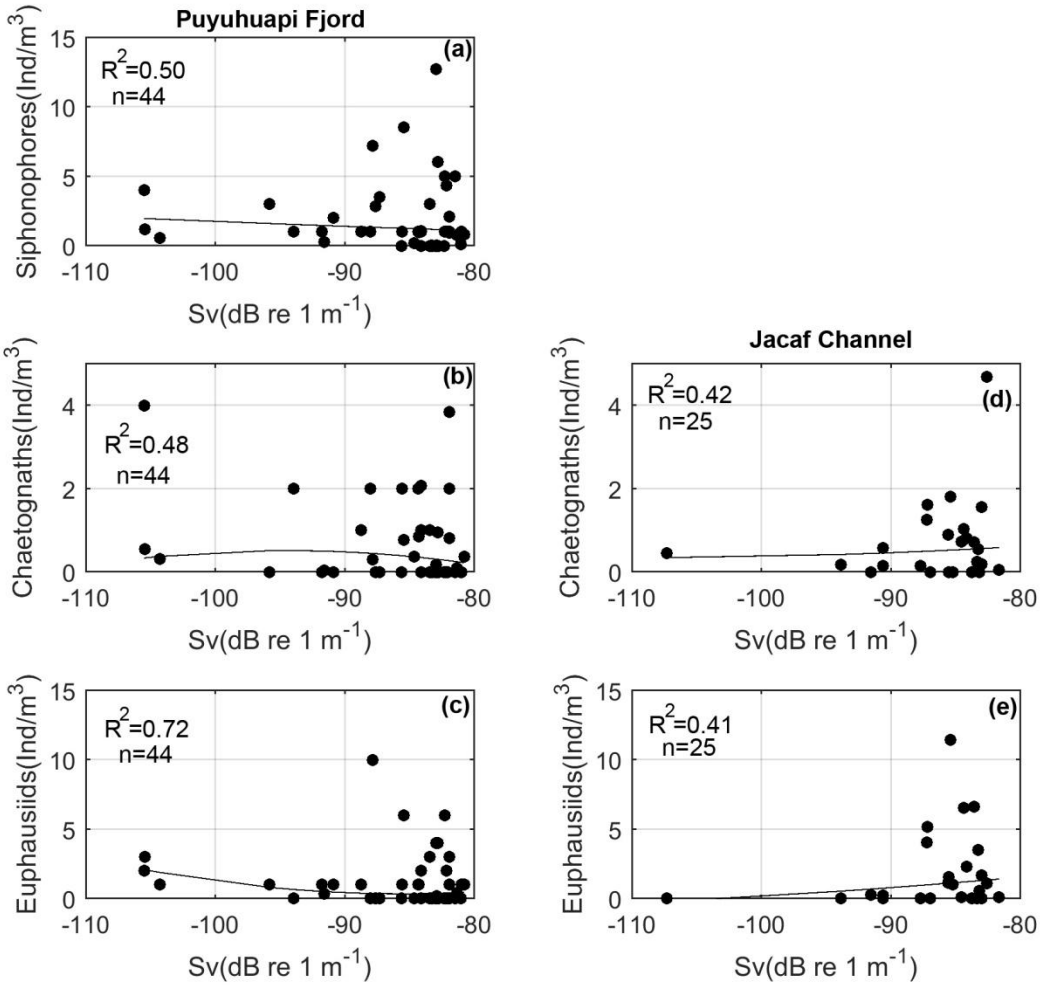

Figure 6. Scatter plot of volume backscattering strength (S_v) from 38 kHz frequency and the most abundance macrozooplankton species obtained in the *in-situ* fixed stations carried out in Puyuhuapi Fjord (a, b and c) during January 22-24, 2014 and (d, e) in Jacaf Channel during August 18-19, 2014.

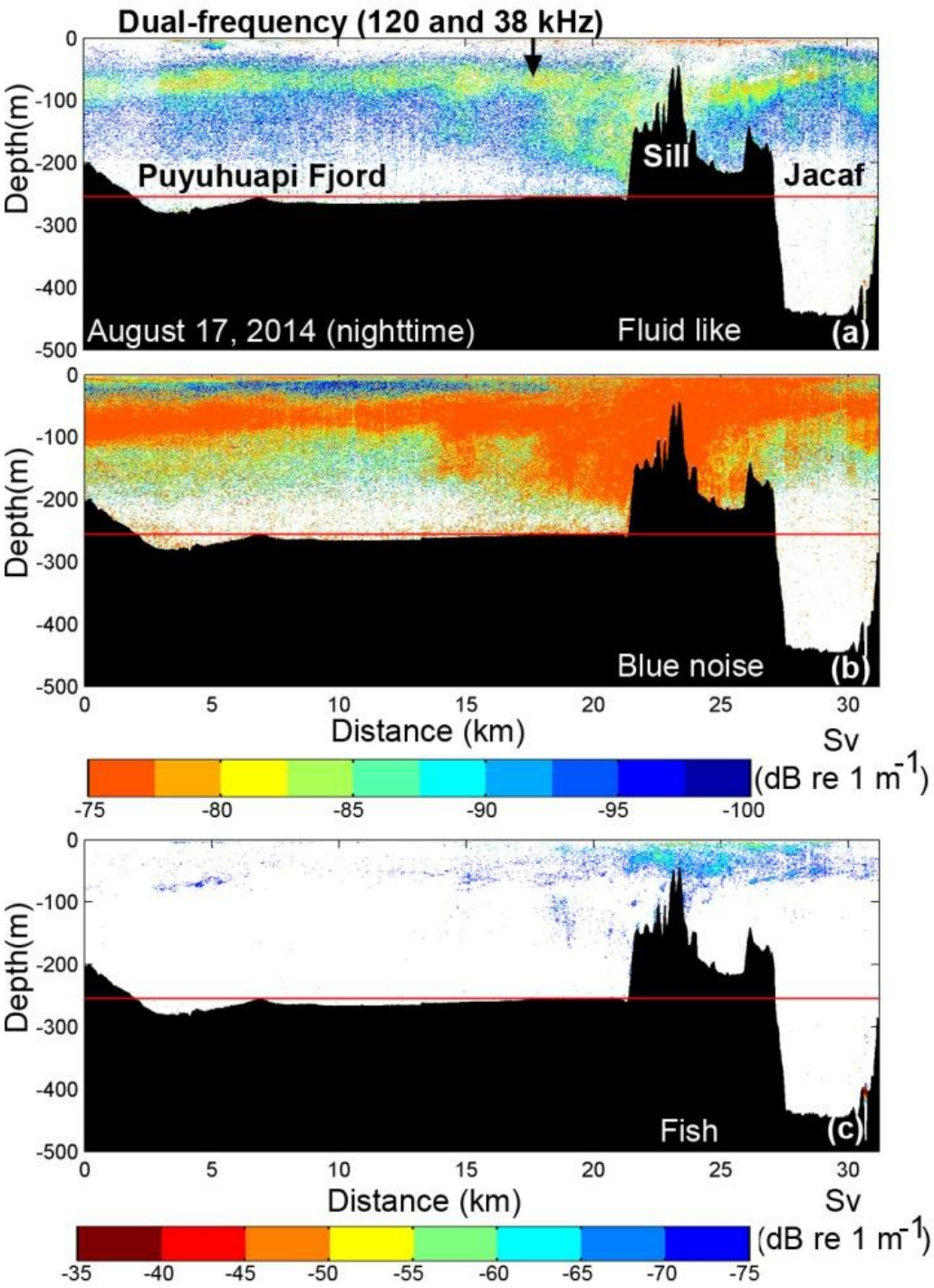

Figure 7. Dual-frequency (38 and 120 kHz) scientific echo-sounder transect along Puyuhuapi Fjord (0-18 km) and Jacaf Channel (18-35 km) during nighttime on August 17, 2014. (a) Fluid like and (b) blue noise echogram for zooplankton and (c) the fish echogram. Distribution indicated by colors representing *Sv* values. The black arrow in (a) represents the entrance to Jacaf Channel. Horizontal red lines in (a, b, c) denote lower limits of usable acoustic data (250 m).

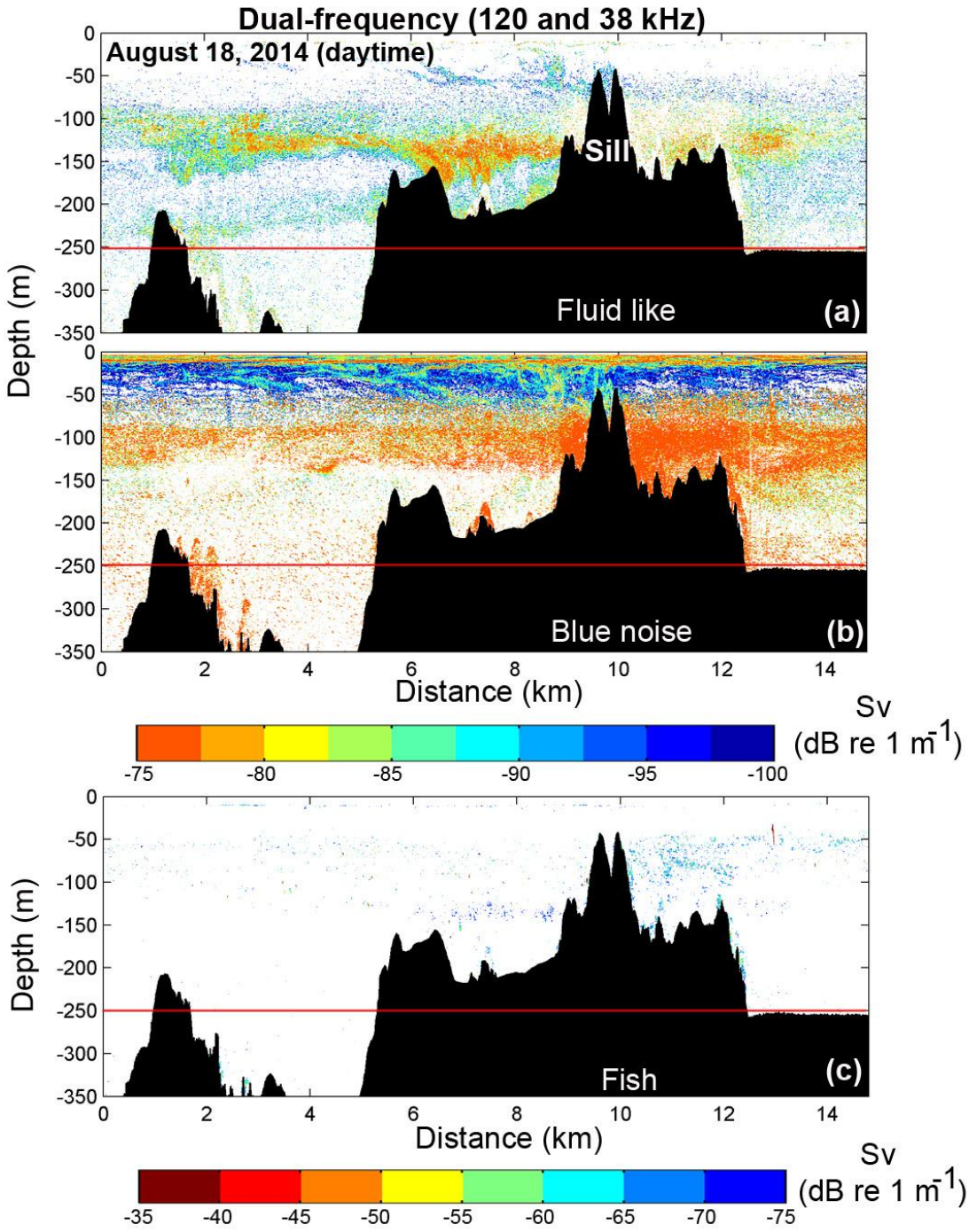

1174

1175 Figure 8. Dual-frequency (38 and 120 kHz) acoustic transect across the Jacaf sill conducted
1176 during daytime on August 18, 2014. (a) Fluid-like echogram, (b) blue noise echogram for
1177 zooplankton and (c) the fish echogram. Distribution indicated by colors representing S_v
1178 values. Horizontal red lines in (a, b, c) denote lower limit of usable acoustic data (250 m).

1179

1180

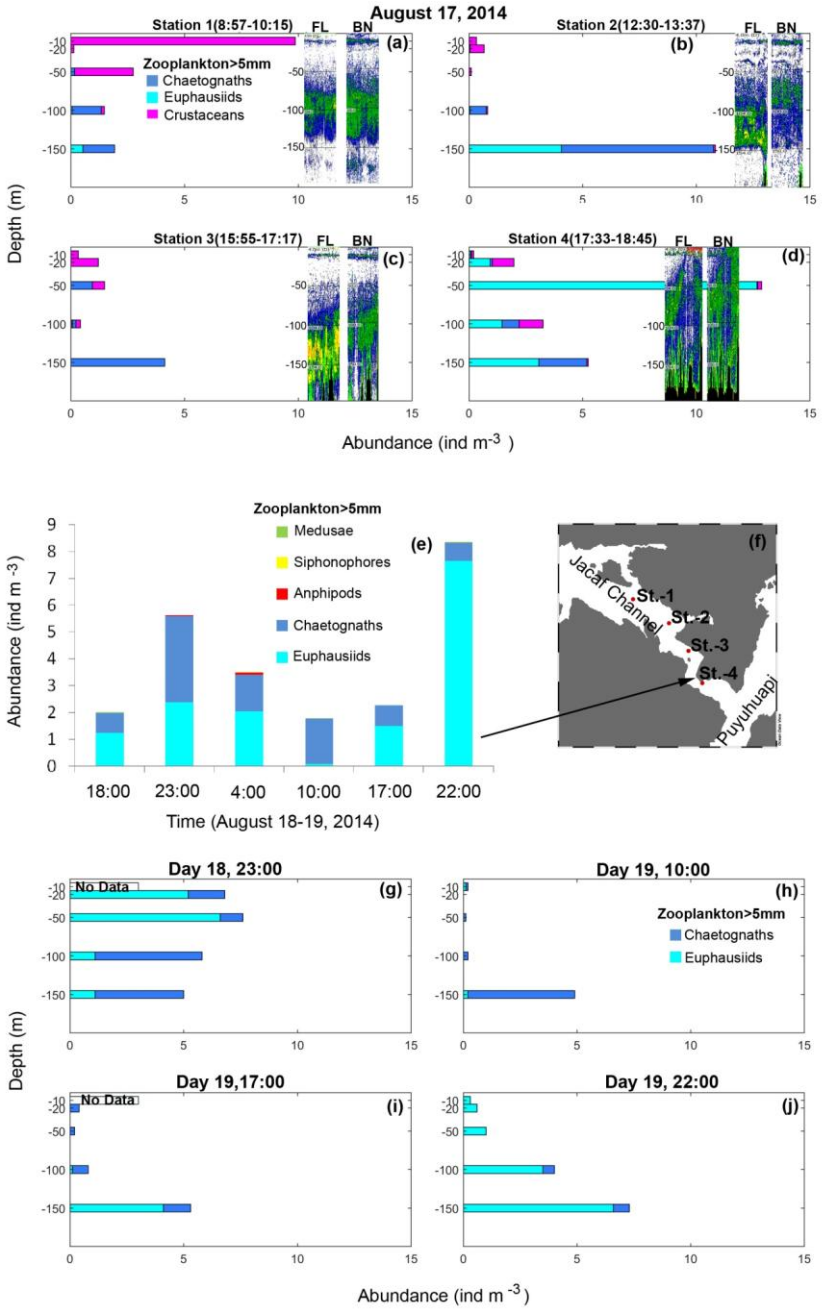

1181

1182 Figure 9. (a-d) *In-situ* stratified zooplankton sampling along Jacaf Channel during August 17,
1183 2014 and the acoustic data collected simultaneously using the dual-frequency (38 and 120
1184 kHz). FL is fluid-like and BN is blue noise groups. (e) Depth integrated abundance of
1185 macrozooplankton groups from surface to 150 m depth for various sampling hours. (f)
1186 Showed the stations positions. (g-j) The vertical abundance of the main macrozooplankton
1187 groups found during the wintertime survey.

1188

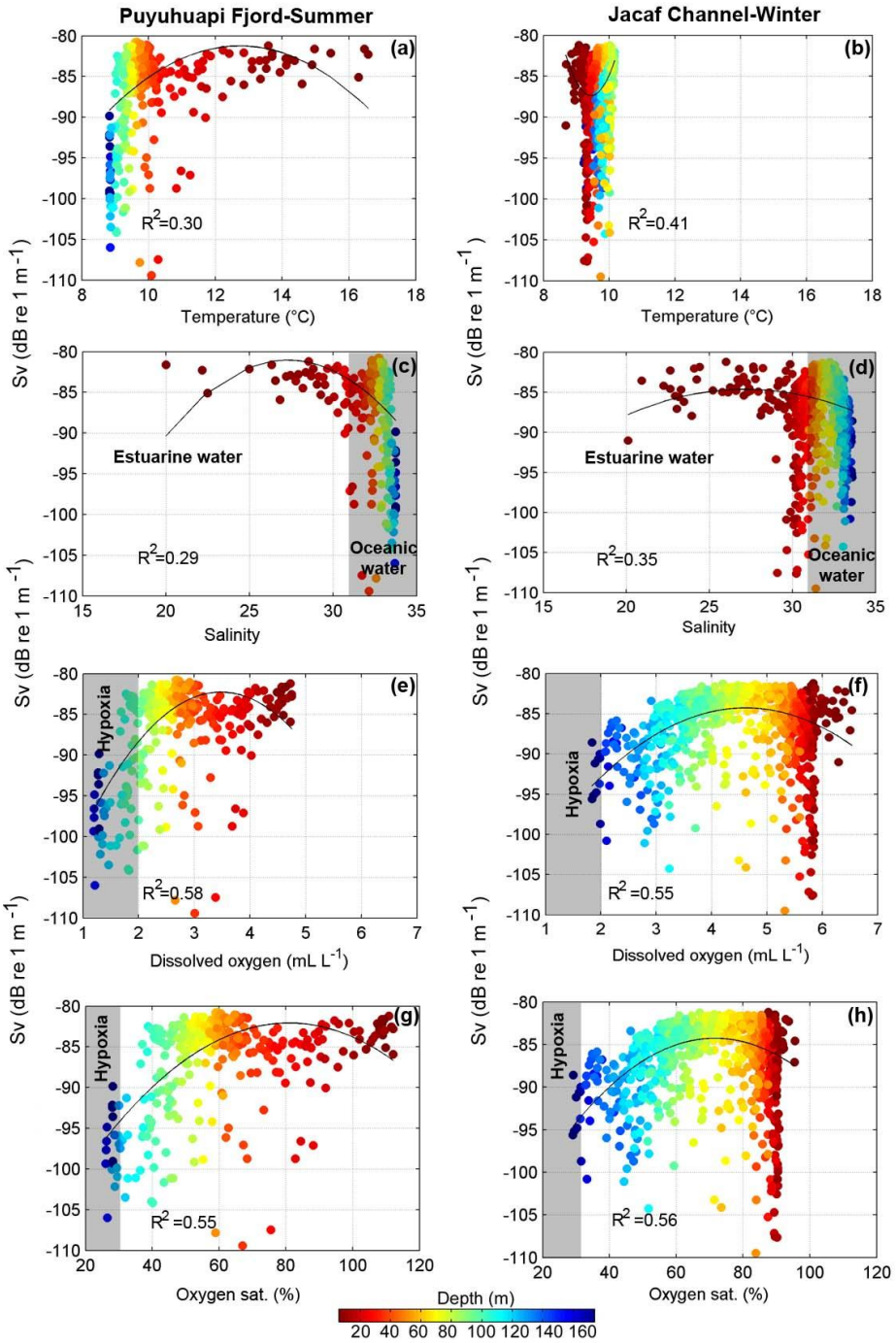

Figure 10. Relationships between the relative abundance of zooplankton (expressed in S_v values) using 38 kHz frequency echo-sounder measurements (*y*-axis) and temperature in (a) Puyhuhuapi Fjord and (b) Jacaf Channel; salinity in (c) Puyuhuapi Fjord and (d) Jacaf Channel; dissolved oxygen in (e) Puyuhuapi Fjord and (f) Jacaf Channel; oxygen saturation in (g) from Puyuhuapi Fjord and (h) Jacaf Channel. The black lines denote the quadratic fit curves, contour colors indicate depth.

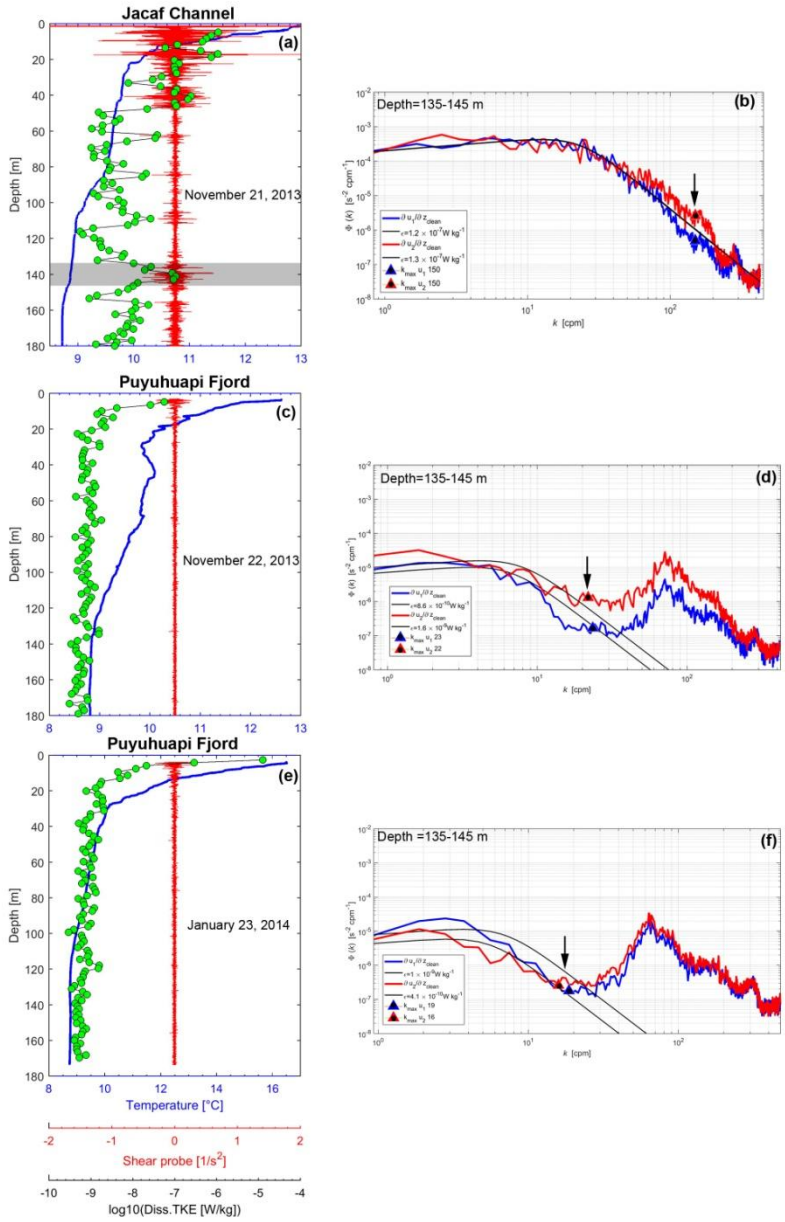

Figure 11. Profiles of water temperature (blue line), vertical shear (red line) and dissipation rate of turbulent kinetic energy (black line with green dots) obtained with the VMP-250 microprofiler at the depth of the Jacaf sill (~140 m depth) in (a) Jacaf Channel on 21 November 2013 (c) Puyuhuapi Fjord on 22 November 2013 and (e) in Puyuhuapi Fjord on 23 January 2014. (b, d, f) Reprentative spectrum of velocity shear ($\partial u/\partial z$) for shear probe 1 (blue line) and 2 (red line) in wavenumber space in Jacaf Channel on 21 November 2013, Puyuhuapi Fjord on 22 November 2013 and Puyuhuapi Fjord on 23 January 2014, respectively. The black line denotes the dimensional Nasmyth spectrum and the red and blue triangles the cut-off of maximum wavenumber (k_{max}) for each shear probe. The shear spectrums were carried out in the same layer (135-145 m) for all turbulence profilers.

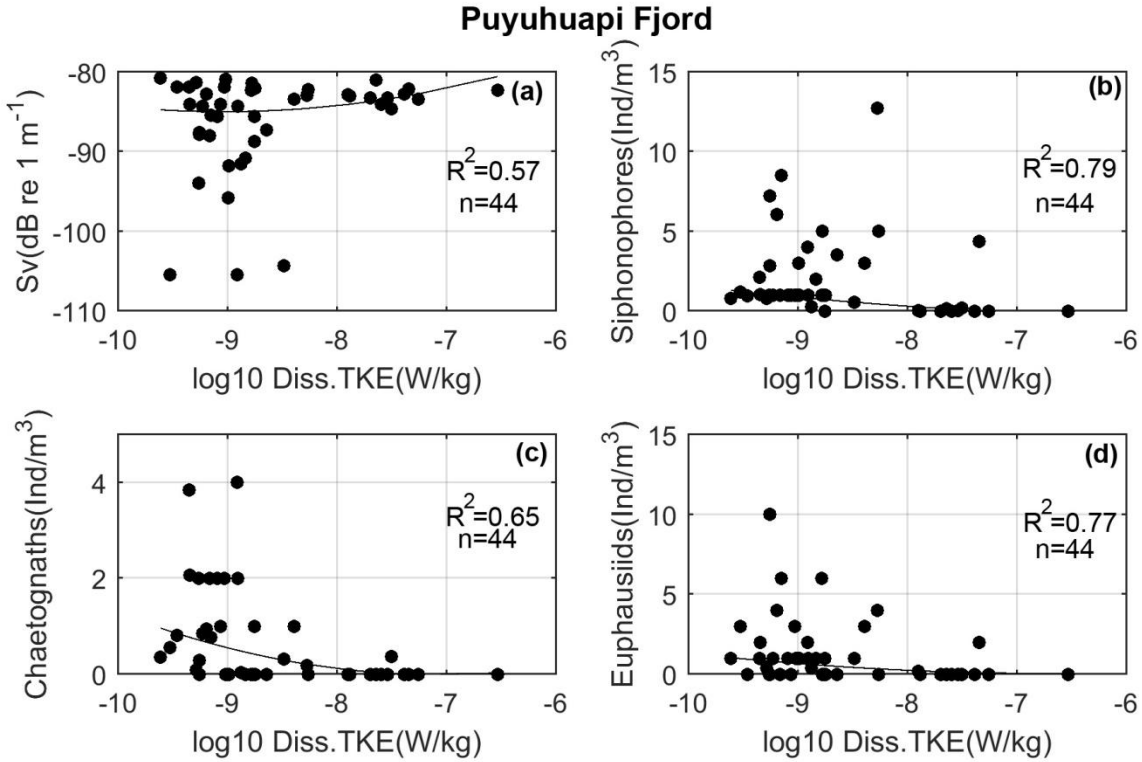

1207

1208 Figure 12. Scatter plot of dissipation rate of turbulent kinetic energy (ε) and (a) volume
1209 backscattering strength (S_v) from 38 kHz frequency and (b, c and d) the most abundance
1210 macrozooplankton species obtained in the *in-situ* fixed stations carried out in Puyuhuapi Fjord
1211 during January 22-24, 2014.

1212

1213

1214

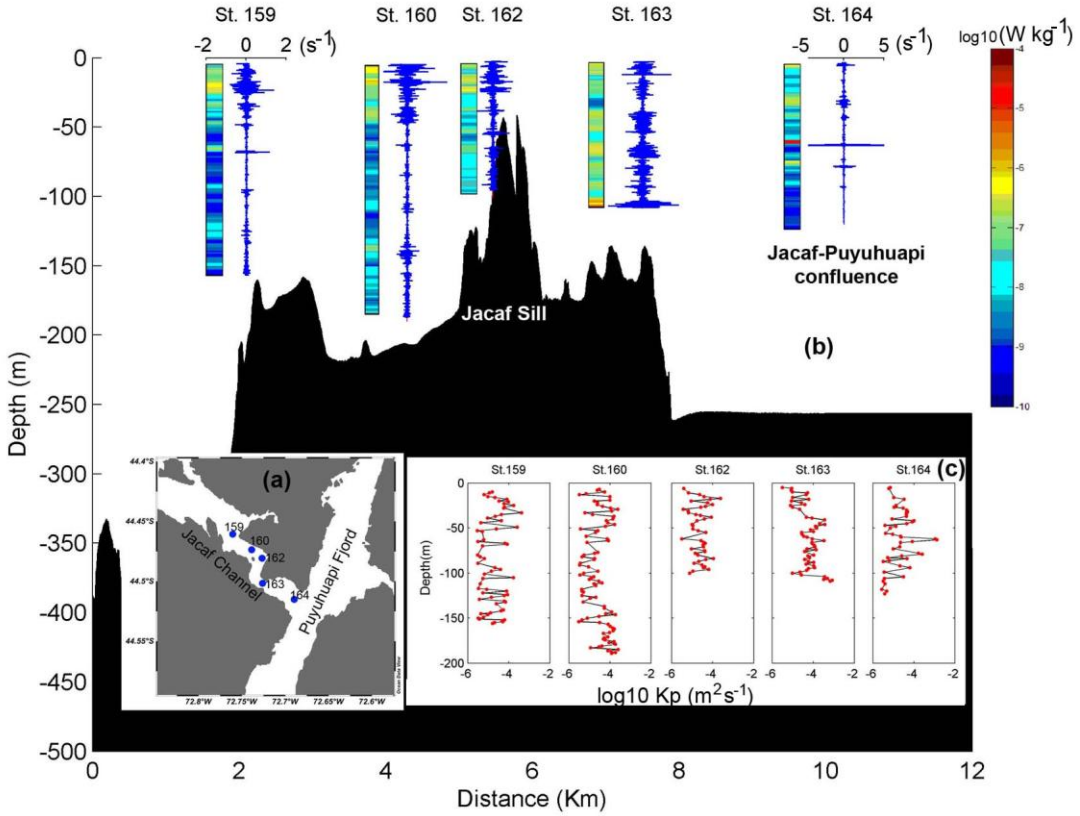

Figure 13. (a) Microstructure profile locations along Jacaf Channel and sill using VMP-250 in November 2013. (b) The color bar showed the dissipation rate of turbulent kinetic energy (ε) and the blue lines depict the velocity shear at each station location along Jacaf Channel (as shown in (a). The horizontal scale (-2 to 2 s^{-1}) applied to profiles at stations 160, 162 and 163. Station 164 is located at the confluence of Jacaf Channel and Puyuhuapi Fjord (10.5 km) (c) The diapycnal eddy diffusivity profiles (K_p), obtained at each station shown in (a).

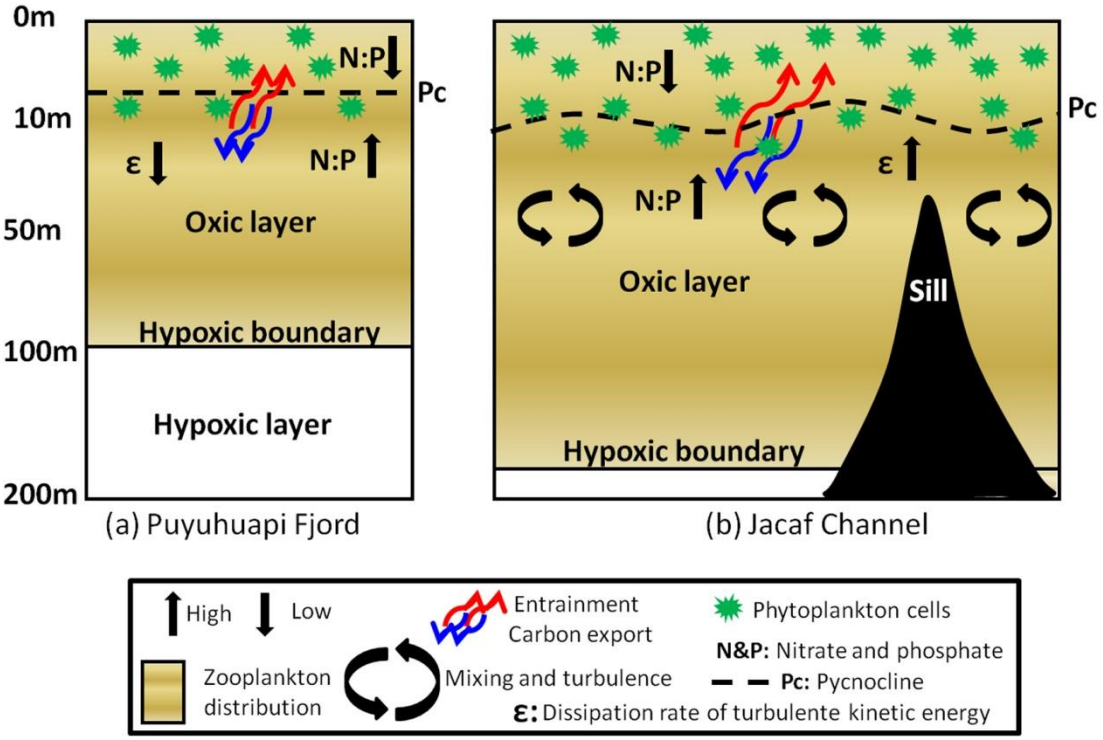

Figure 14. Conceptual model to show the oceanographic processes that contribute to the distribution and aggregation of zooplankton in (a) Puyuhuapi Fjord and (b) Jacaf Channel.

Table 1. Data set collected during oceanographic campaigns in Puyuhuapi Fjord and Jacaf Channel.

Location	Date	Season	Data measured	Instruments
Puyuhuapi Fjord	May 8-27, 2013	Fall	-Acoustic data 307.7 kHz	-ADCP-1 RDI
			-Zooplankton	-WP2 net
			-Hydrography	-CTD SBE-25
			-Nitrate	Spectrophotometry
	November 22, 2013	Spring	-Turbulence	-VMP-250
			-Hydrography	-CTD SBE-25
	January 22-25, 2014	Summer	-Acoustic data 307.7 kHz	-ADCP-2 RDI
			-Acoustic data 38 kHz	-SIMRAD EK60
			-Zooplankton	-Tucker Trawl net
			-Turbulence	-VMP-250
			-Hydrography	-YSI 6600
			-Nitrate	Spectrophotometry
	August 17-19, 2014	Winter	-Acoustic data 38 and 120 kHz	-SIMRAD EK60
			-Zooplankton	-Tucker Trawl net
			-Hydrography	-CTD SBE-25

			-Nitrate	Spectrophotometry
	February-June 2016	Summer-Fall	-Tidal data (south)	-HOBO U20
	February-November 2016	Summer-Spring	-Tidal data (north)	-HOBO U20
	June 16, 2016	Fall	-Hydrography	-CTD SBE-25
Jacaf Channel	April-November 2012	Fall-Spring	-Tidal data	-HOBO U20
	November 21, 2013	Spring	-Turbulence	-VMP-250
			-Hydrography	-CTD SBE-25
	August 2014-May 2015	Winter-Spring–Summer-Fall	-Tidal data	-ADCP-3
	August 17-19, 2014	Winter	-Acoustic data 38 and 120 kHz	-SIMRAD EK-60
			-Zooplankton	-Tucker Trawl net
			-Hydrography	-CTD SBE-25

1230

1231 Table 2. Harmonic analysis implemented to water level time series in Puyuhuapi Fjord and
1232 Jacaf Channel.

1233

Sea level time series	**Date (mm-yyyy)**	**Energy from semi-diurnal band (m^2 cph^{-1})**	**Amplitude of principal constituents (cm)**				**F**	**Tidal regime**
			M_2	**S_2**	**O_1**	**K_1**		
Jacaf-HOBO	04-09/2012	45.10	83.45	28.32	14.46	22.33	0.32	Mixed semi-diurnal
Jacaf-ADCP	08/2014-05/2015	57.29	60.67	61.01	57.78	42.48	0.82	Mixed semi-diurnal
Puyuhuapi-HOBO south	02-06/2016	44.45	81.97	31.51	13.37	18.36	0.27	Mixed semi-diurnal
Puyuhuapi-HOBO north	02-11/2016	49.17	89.15	31.07	11.03	17.75	0.23	Semi-diurnal

1234